Israel Journal of Chemistry / Volume 62, Issue 1-2 / e202100071

Review | Full Access

Computations on Pericyclic Reactions Reveal the Richness of Ambimodal Transition States and Pericyclases

K. N. Houk, Xiao-Song Xue, Fang Liu, Yu Chen, Xiangyang Chen, Cooper Jamieson

First published: 02 September 2021
https://doi.org/10.1002/ijch.202100071
Citations: 1

Abstract

The pericyclic reaction concept was developed by Woodward and Hoffmann 56 years ago, before accurate quantum mechanical calculations of organic reaction pathways were possible. Since then, computational methods such as density functional theory and coupled-cluster methods have been formulated, and computer speeds have increased a hundred trillion (10^{11})-fold. The subtleties and timings of bond formation in reactions have been established by high-accuracy quantum mechanical calculations. The field of pericyclic reactions has been enriched by understanding of the borderline between concerted pericyclic reactions and stepwise reactions. Higher-order pericyclic reactions, involving more than six electrons, have ambimodal transition states that can form two, three, or even four products. In addition, while only imagined in the last century, the fact that enzymes can catalyze many pericyclic reactions has been repeatedly established in the 21st century, aided enormously by computational studies.

1 Introduction

This article is about the impact of modern computational chemistry – especially quantum mechanics – on one important area of chemistry, the field of pericyclic reactions, a large family of organic reactions occurring in one concerted step. Our manuscript describes what has become common in chemistry – the ability of computations to bring depths of insight not

previously feasible from pure experiment. The rise of computation has been accompanied by enormously accelerated discovery by experiment, due to modern instrumentation and the expansion of the scientific workforce.

The article begins with the definition of pericyclic reactions and a brief discussion of the state of understanding of reaction mechanisms in the mid-twentieth century, at the very beginning of the use of quantum mechanical calculations to study reaction mechanisms. The article then turns to a more detailed discussion of one area of pericyclic reactions, cycloadditions. An area of frequent discussion and disagreement about mechanism based on experimental evidence, cycloaddition mechanisms have gained new clarity and, indeed, a whole new classification, ambimodal mechanisms, due to the development of high accuracy calculations. Finally, the discoveries of such reactions in enzyme-catalyzed reactions of biosynthesis are described.

In the mid-twentieth century, organic reaction mechanisms were investigated by the experimental tools available at the time: kinetics, isotope effects, and identification of intermediates by spectroscopic means. Classifications of mechanisms were rather coarse: S_N1 versus S_N2, stepwise versus concerted, diradical versus zwitterionic.[1] There were attempts to introduce more subtlety into these descriptions: Winstein's 1949 proposal that the acceleration of the solvolysis of exo-norbornyl derivatives occurs with development of a delocalized "nonclassical" cation[2] is one early example of this type. The 1959 Woodward-Katz proposal of the "two-stage" mechanism of Diels-Alder reactions of two dienes[3] is another example more directly relevant to the subject of this article.

Perhaps the first serious attempt to understand mechanisms and the nature of transition states with theory was Fukui's frontier molecular orbital theory[4] and Woodward and Hoffmann's proposals about the conservation of orbital symmetry. In a series of communications, and then the *Angewandte Chemie* review that became a book, "The Conservation of Orbital Symmetry,"[5] the concept of pericyclic reactions was established.

The key feature of pericyclic reactions is that they are concerted – one transition state – with all bonding changes occurring together on a ring. Only certain arrangements maintain maximum bonding along the concerted pathway, and these are the allowed pericyclic reactions. Woodward and Hoffmann defined which combinations of stereochemistries and numbers of electrons involved in bonding changes lead to favorable (allowed) reactions. For cycloadditions, electrocyclizations, sigmatropic shifts, and a few others with cyclic delocalized transition states, the Woodward-Hoffmann rules tell us what reactions are preferred.[5]

Computational methods available at the time, especially the early *ab initio* calculations with Hartree-Fock theory and small basis sets, and the semi-empirical methods promoted by Dewar, did not always agree on the nature of the transition states of potentially pericyclic reactions.

Some of the controversies about whether pericyclic reactions really are concerted are described in one of our *Accounts of Chemical Research* articles of the time.[6]

In the meantime, better and better methods of computation, including density functional theory and much faster computers (trillion times faster now than when the Woodward-Hoffmann rules were devised), vastly improved instrumentation and methods for kinetics and identification of intermediates, and the routine use of computer-intensive molecular dynamics methods, have led to the discoveries of many details about the potential surfaces and timing of bonding changes in pericyclic reactions.[7] All of these advances have led to the discoveries described in the remainder of this article.

2 Subtleties of Mechanism Revealed by Quantum Mechanics and Molecular Dynamics

2.1 Ambimodal Polypericyclic Reactions

2.1.1 Ambimodal 6+4/4+6 Cycloadditions

In 1965, the [6+4] cycloaddition was predicted to be an orbital symmetry allowed pericyclic reaction under thermal conditions by Woodward and Hoffmann (Figure 1).[9]

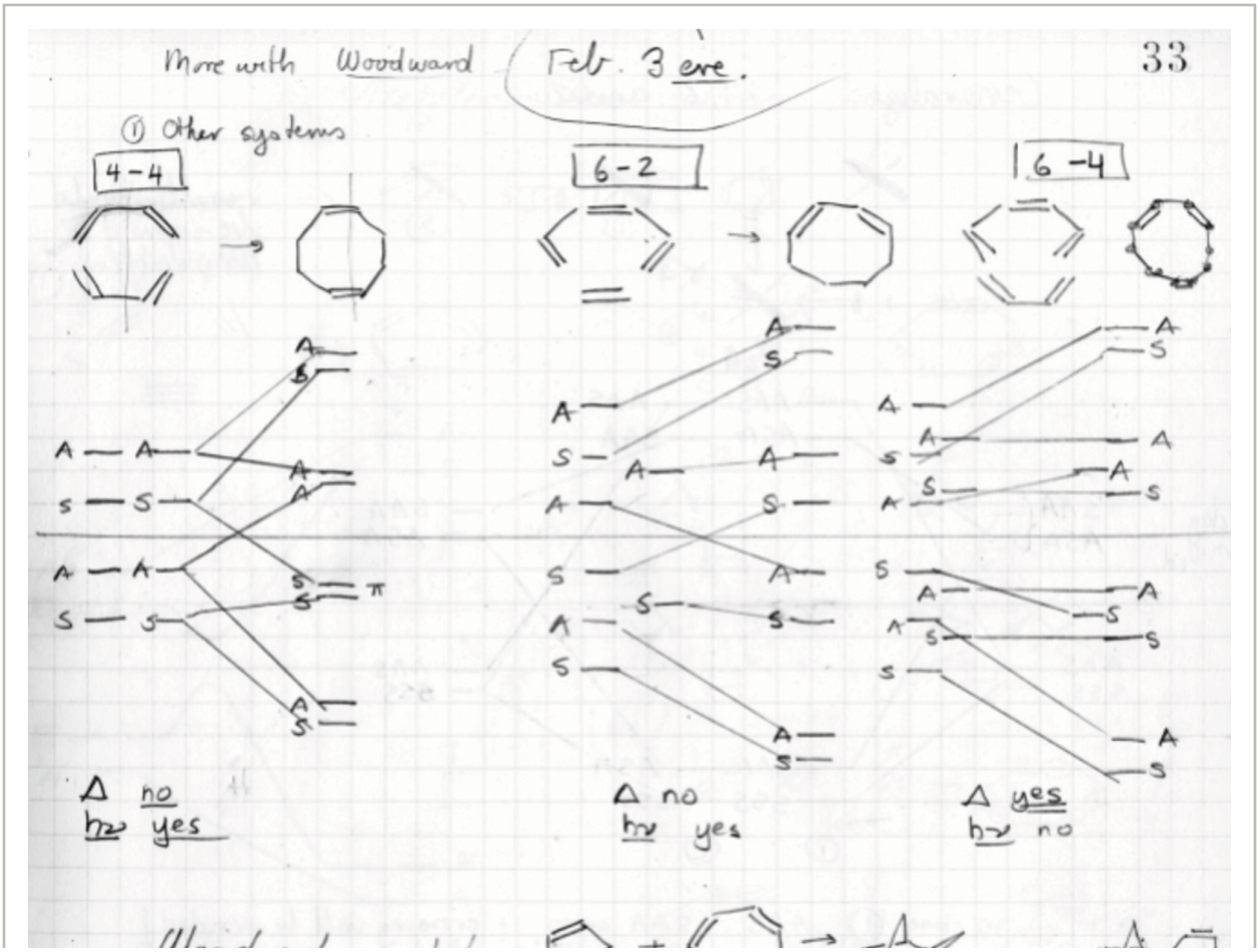

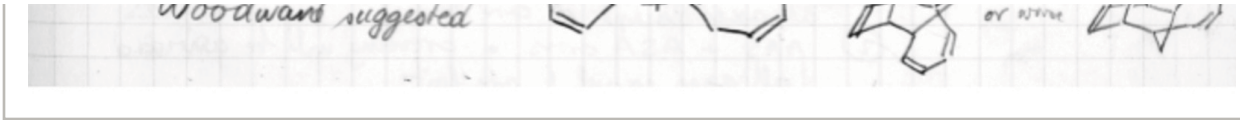

Figure 1 Open in figure viewer | PowerPoint

Page 33 from notebook 16, dated February 3, 1965, by Hoffmann where the orbital correlation diagrams for [4+4], [6+2], and [6+4] cycloadditions were first described. Below these is a suggestion by Woodward of a [6+4] cycloaddition of cyclopentadiene with cycloheptatriene.[8] This became Houk's first research project in graduate school. (This figure reprinted by permission of the American Chemical Society.)

The search for [6+4] cycloadditions then become the first research project of author K. N. Houk while working on his Ph.D. with R. B. Woodward. A series of [6+4] cycloadditions were discovered by Houk in the Woodward lab,[10] but some of the products were too complex for methods and instrumentation of the period. A notable [6+4] cycloaddition is the reaction between dimethylfulvene [6π] and tropone [4π], which was studied experimentally by Houk as a graduate student in the Woodward lab and first published three years after Houk's Ph.D.[11] This reaction gave a minor amount of a Diels-Alder adduct but mostly a 2 : 1 adduct of dimethylfulvene and tropone along with some of the 1 : 1 adduct (Figure 2A). To explain these observations, Houk proposed a plausible mechanism, involving a [6+4] cycloaddition of dimethylfulvene [6π] to tropone [4π], followed by a [1,5] hydrogen shift to give the thermodynamically more stable cyclopentadiene **4**, which then underwent a second [6+4] cycloaddition with tropone [6π] to form the double [6+4] cycloadduct **3** (Figure 2B). Shortly after, Paddon-Row and Warrener proposed an alternative mechanism: the initial cycloaddition involves a different [6+4] cycloaddition in which fulvene acts as the 4π-component to give **7**.[12] Subsequently, a Cope rearrangement leads to the formal [6+4] adduct **6** (Figure 2B). However, no direct experimental evidence could be obtained to prove either mechanism, and that is how the matter would have ended were it not for the development of computations.

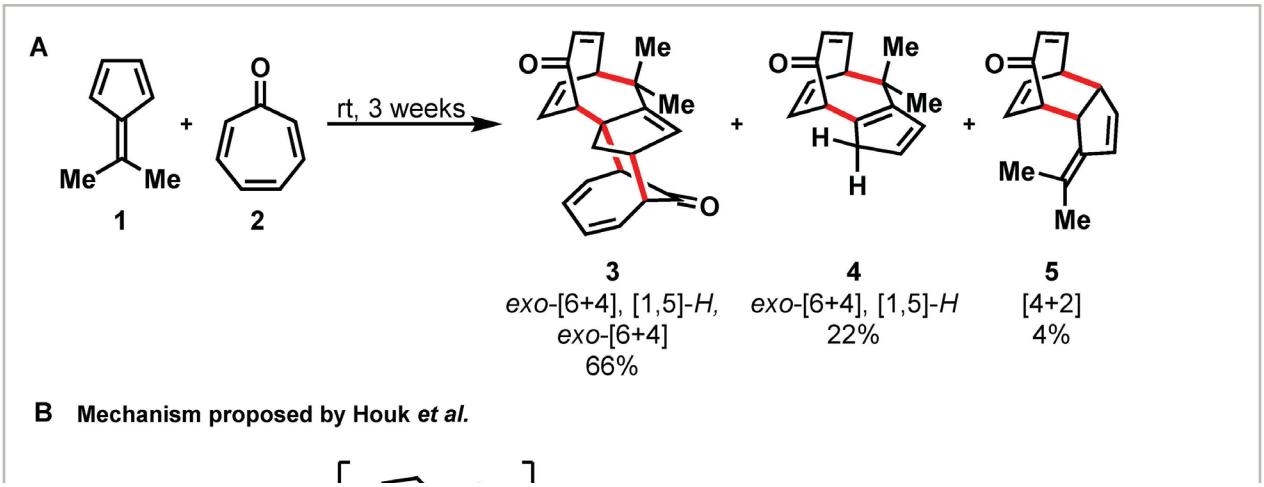

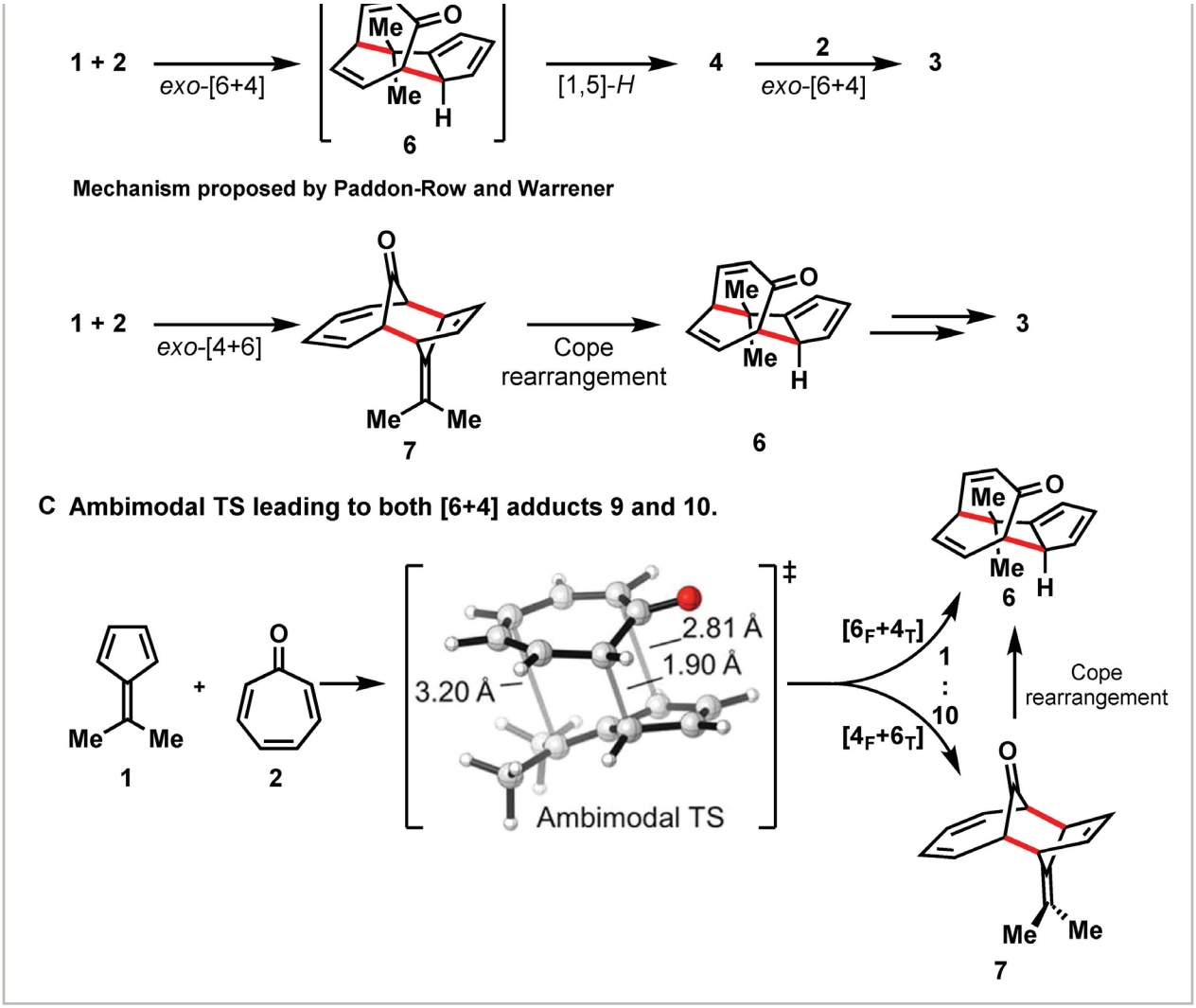

Figure 2

Open in figure viewer | PowerPoint

A. Product distribution of the reaction between fulvene **1** and tropone **2. B**. Mechanistic proposals for the formation of product **3. C**. Ambimodal TS leading to both [6+4] adducts **6** and **7**. (This figure by permission of the American Chemical Society.)

In 2017, Houk and coworkers revisited the mechanism and periselectivity of the [6+4] cycloaddition of tropone to dimethylfulvene with density functional theory (DFT) calculations and quasi-classical direct molecular dynamics simulations.[13] Computations revealed that the reaction proceeds via a Woodward-Katz two-stage process but involves a single ambimodal transition state that can lead to both of the proposed [6+4] adducts **6** and **7** (Figure 2C) without formation of an intermediate. These adducts can interconvert through a Cope rearrangement, and the observed product is the thermodynamically more stable adduct. An "ambimodal"[14] "bipericyclic"[15] transition state can lead to multiple products without intervening minima or secondary barriers to overcome. (Note that we use bi-pericyclic for two different competing pericyclic reactions from one transition state, while Caramella used bis-pericyclic to described

two identical cyclopentadiene reactants undergoing two identical reactions.) The occurrence of such a transition state is a result of a post-transition state bifurcation (PTSB).[16] In such circumstances, the rate of a reaction can still be predicted by transition state theory, while the product distribution is dynamically controlled. Quasi-classical direct molecular dynamics simulations provide an ideal tool to study such bifurcating reactions. Such dynamics simulations not only predict the distribution of products for bifurcating reactions, but also provide valuable information on the time-resolved mechanisms. For the [6+4] cycloaddition of tropone to dimethylfulvene, 91 % of the trajectories go to adduct **7**, while 9 % trajectories lead to adduct **6**, suggesting that both adducts are formed initially in the reaction, but there is a dynamic preference (10 : 1) for the formation of **7** over **6**, the Paddon-Row-Warrener mechanism. This showcases that the quantum mechanical modelling methodologies are invaluable for the deduction of the mechanism of pericyclic reactions that are challenging or impractical to study via experimental means.

The concerted/stepwise dichotomy in Diels-Alder reactions has been the subject of a long-standing debate.[6] Modern computations demonstrate, however, that the borderlines between concerted, two-stage, and stepwise are blurred. During systematic molecular dynamics studies of cycloaddition reactions, Houk and colleagues proposed a timing criterion to differentiate between dynamically stepwise and dynamically concerted mechanisms.[17] The mechanism is considered to be dynamically concerted if all bonding changes are complete in less than 60 fs, but dynamically stepwise otherwise. The criterion was defined from the lifetime of the TS derived from Eyring's TS theory. Analysis of the trajectories for the [6+4] cycloaddition of tropone to dimethylfulvene showed that the time gaps of trajectories leading to cycloadducts **6** and **7** are at the borderline between dynamically concerted and a dynamically stepwise mechanisms.[18]

Most reported ambimodal transition states (TS) refer to single bifurcations, leading to only two sets of different products without an intervening minimum. Very recently, Houk's group discovered the first example of ambimodal tripericyclic TS that can lead to three different products by using DFT computations and quasi-classical direct molecular dynamics simulations.[19] They found that transition states for the reaction between electron-deficient 8,8-dicyanoheptafulvene **8** with dimethylfulvene **1**,[20] which was reported by C.-Y. Liu (Houk's graduate student who became a professor in Taiwan) in 1992, can lead to [4+6]-, [6+4]-, and [8+2]-cycloadducts. This occurs by all trajectories going through one TS, bifurcating to two other pathways, and then each of these paths bifurcates again. Trajectories initiated from **TS** lead to three different cycloadducts (Figure 3). The dynamics show average time-gaps of 90, 74, and 141 fs for formation of [4+6]-, [6+4]-, and [8+2]-cycloadducts, respectively, meaning that this reaction is dynamically stepwise involving entropic intermediates on average. This fascinatingly complicated tripericyclic reaction broadens our knowledge of pericyclic

ambimodality.

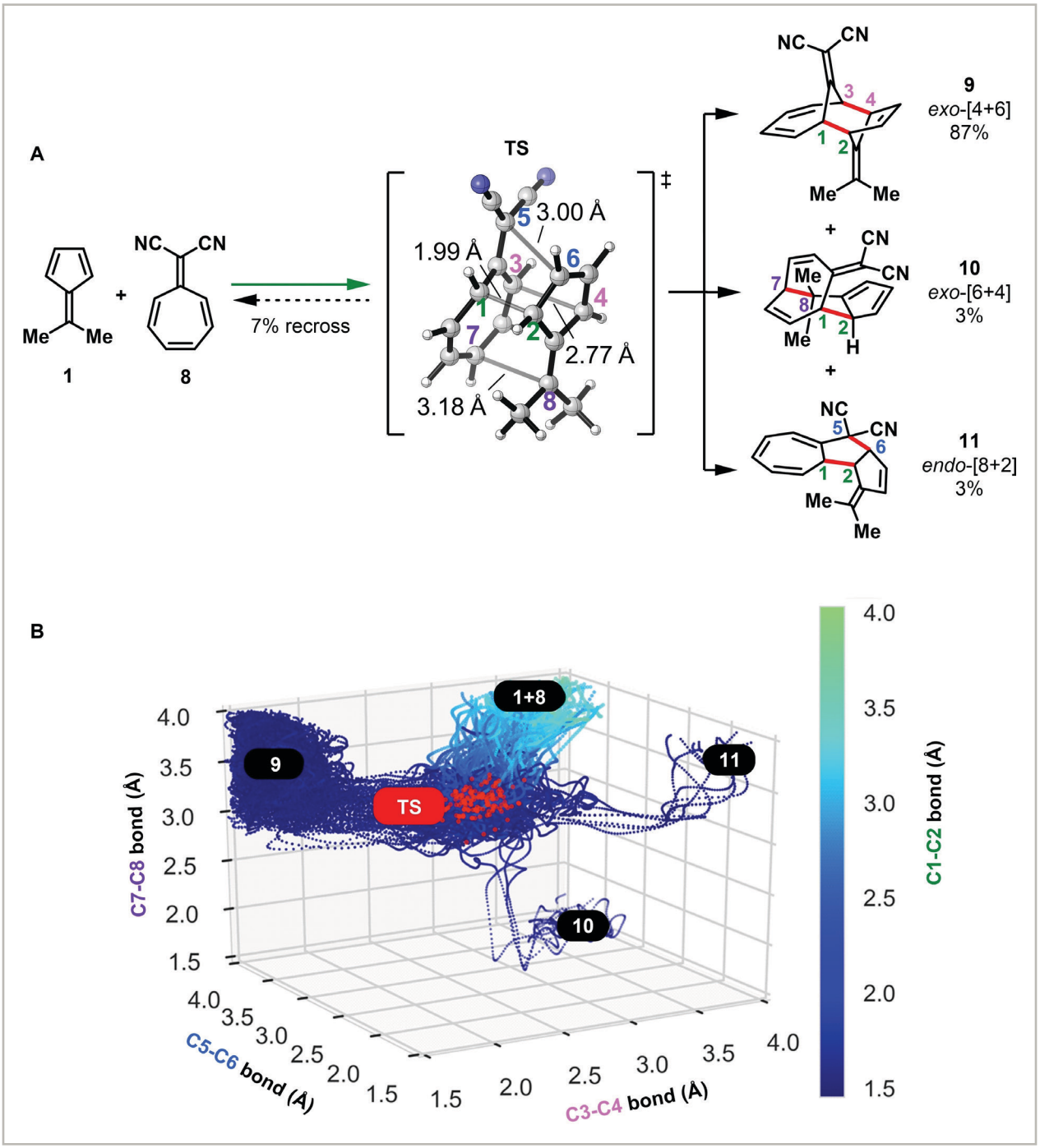

Figure 3

Open in figure viewer | PowerPoint

A. Theoretical product distribution of a tripericyclic reaction (molecular dynamics yields). **B**. Trajectories initiated from **TS**; color codes the length of the forming C1–C2 bond present in all products, while the x, y, and z axes are for the conditional primary interactions leading to three products.

Most recently, Houk's group pushed the limits even further by designing an ambimodal

transition structure (TS) for a cycloaddition reaction that directly connects to four different cycloadducts – [4+6], [2+8], [8+2], and [6+4] – via multiple bifurcations involving transition states lower in energy than the tetrapericyclic transition state (Figure 4).[21] It is still unclear how far one could go for the search of multiple bifurcations.

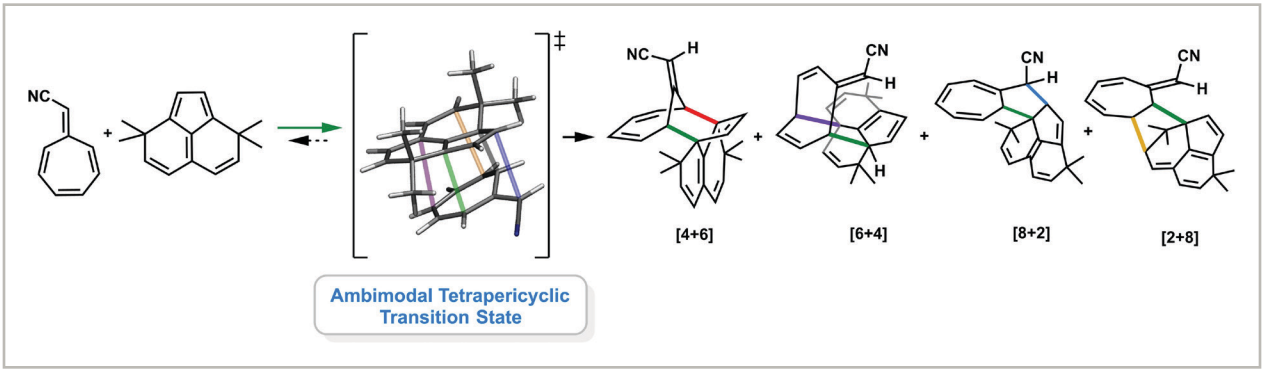

Figure 4 Open in figure viewer | PowerPoint

A tetrapericyclic reaction with an ambimodal tetrapericyclic transition structure **TS1** leading to [4+6]-, [2+8]-, [8+2]-, and [6+4]-cycloadducts.

Clearly, the quantum mechanical modelling methodologies have provided significant new insights into the mechanism and periselectivity of higher-order cycloadditions, which in turn could help the design of new cycloadditions with high periselectivity. An attractive and exciting area of research is to modulate the ambimodal tetrapericyclic transition structure that enables access to complex ring systems which are difficult to obtain by other means.[22]

2.1.2 Ambimodal Dipolar Cycloaddition

2.1.2.1 [4+2] 1,3-Dipolar Cycloadditions

In 1960, the 1,3-dipolar cycloaddition was announced by Rolf Huisgen in his famous Centenary Lecture.[23] He defined the general form of 1,3-dipoles, represented by XYZ as shown in Figure 5. In 1968, Huisgen defined cycloadditions in terms of the atoms involved in forming the ring. The 1,3-dipolar cycloaddition is called a (3+2) cycloaddition in those terms.[24] In terms of electrons involved in bonding changes, the nomenclature proposed by Woodward and Hoffmann, this is also a [4+2] cycloaddition. This reaction is an important method for the synthesis of heterocycles.

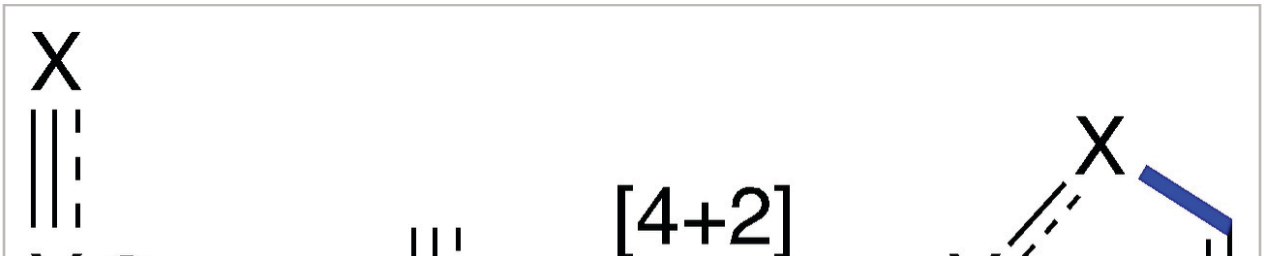

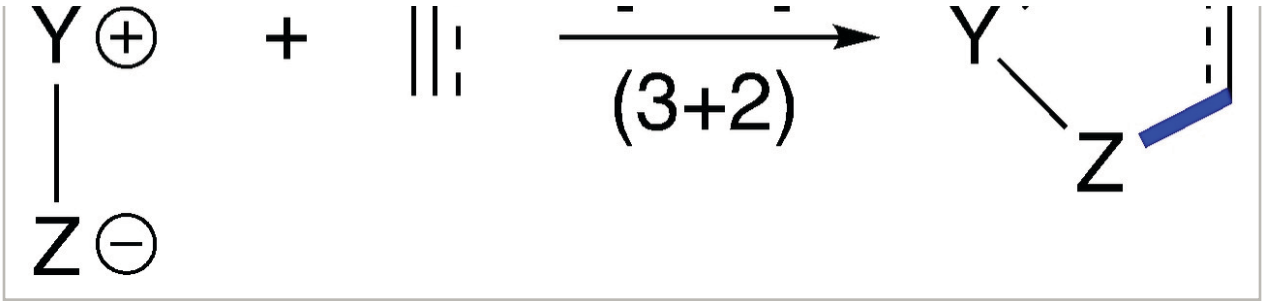

Figure 5 Open in figure viewer | PowerPoint

The [4+2] 1,3-dipolar cycloadditions to alkenes or alkynes.

2.1.2.2 [6+4] 1,3-Dipolar Cycloadditions

In 1965, Woodward and Hoffmann first predicted that trienes could react with dienes in a [6+4] fashion based on the Woodward-Hoffmann rule.[25] As described above, this was also proved experimentally. We wondered if this kind of reaction could also occur with 1,3-dipoles (4 electron) and trienes (6 electrons) (Figure 6). This led to the experimental studies in various groups and our recent computational studies to establish the mechanisms of these reactions.

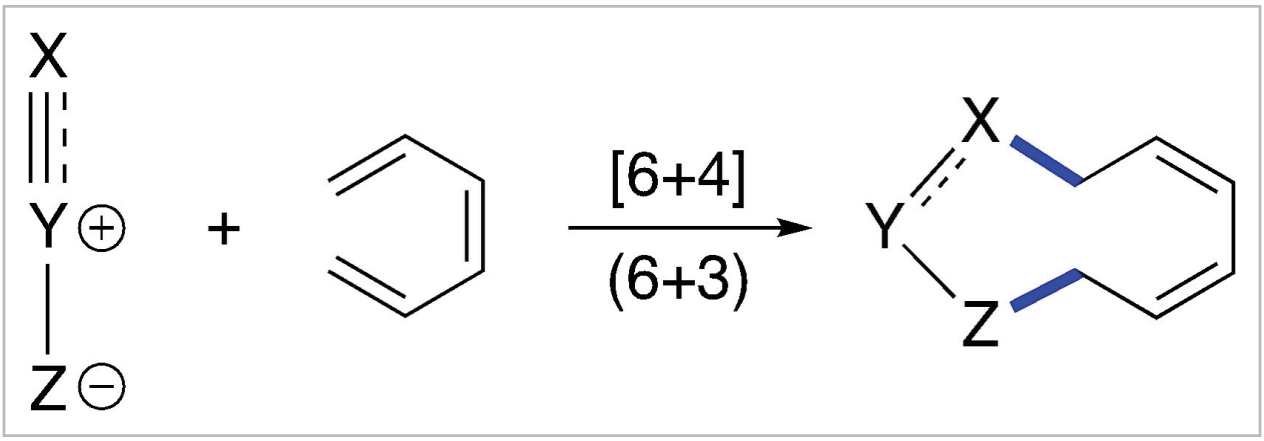

Figure 6 Open in figure viewer | PowerPoint

The [6+4] 1,3-dipolar cycloaddition to trienes.

2.1.2.3 Ambimodal [6+4]/[4+2] 1,3-Dipolar Cycloadditions

The reaction of diazomethane and dimethylfulvene was first studied by Alder *et al*. in 1961, but there was uncertainty about the structures of the products.[26] Alder proposed **13**. In 1970, Houk *et al*. revisited this reaction experimentally and found that a [6+4] adduct was formed. By NMR and UV spectroscopy, product **12** was found to be the product formed in this reaction, and no [4+2] adduct was observed (Figure 7).[27]

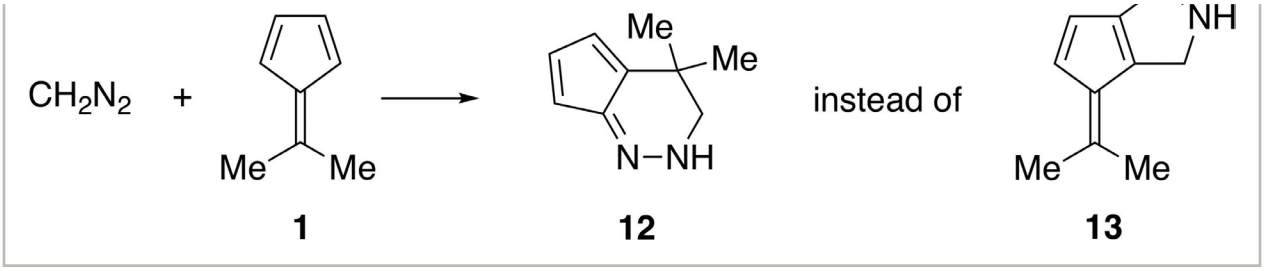

Figure 7 Open in figure viewer | PowerPoint

Diazomethane-dimethylfulvene adducts reported by Alder as **13** and revised to **12** by Houk *et al*.[27]

In 1978, Padwa studied the nitrile ylide cycloaddition to dimethylfulvene, and found that this reaction gave both [6+4] and [4+2] adducts (Figure 8).[28]

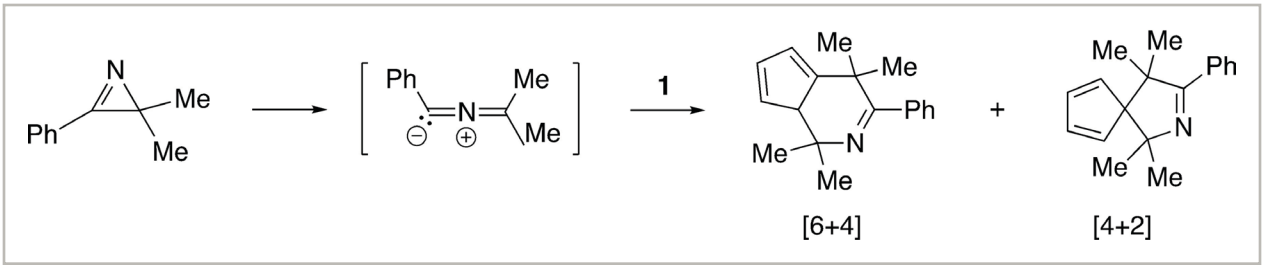

Figure 8 Open in figure viewer | PowerPoint

Padwa's nitrile ylide-dimethylfulvene reaction.

The different outcomes of diazomethane-fulvene and nitrile ylide-fulvene reactions inspired us to investigate the mechanism of these 1,3-dipolar cycloadditions computationally.[29] For the reaction of diazomethane and dimethylfulvene, an ambimodal transition state **TS1** was found, with quite different partial N–C bond lengths, 2.61 Å and 2.98 Å or 2.97 Å, respectively. It appears that this is a rather unique tripericyclic TS, which can actually give three products, the [4+2] adduct and two different [6+4] adducts. Our previous study of the relationship between the differences in partial bond lengths in transition states and the ratios of products obtained by molecular dynamics indicated that, in general, when the difference between the partial bond lengths is greater than 0.4 Å, only one product can be observed in hundreds of molecular dynamics trajectories. Thus, in the case of diazomethane-dimethylfulvene reaction, direct formation of [6+4]-adduct through **TS1** may not occur to a large extent. In fact, this reaction should initially undergo a normal [4+2] 1,3-dipolar cycloaddition to the exocyclic double bond of the fulvene, followed by 1,5-shift and tautomerization to the observed [6+4] product (Figure 9).

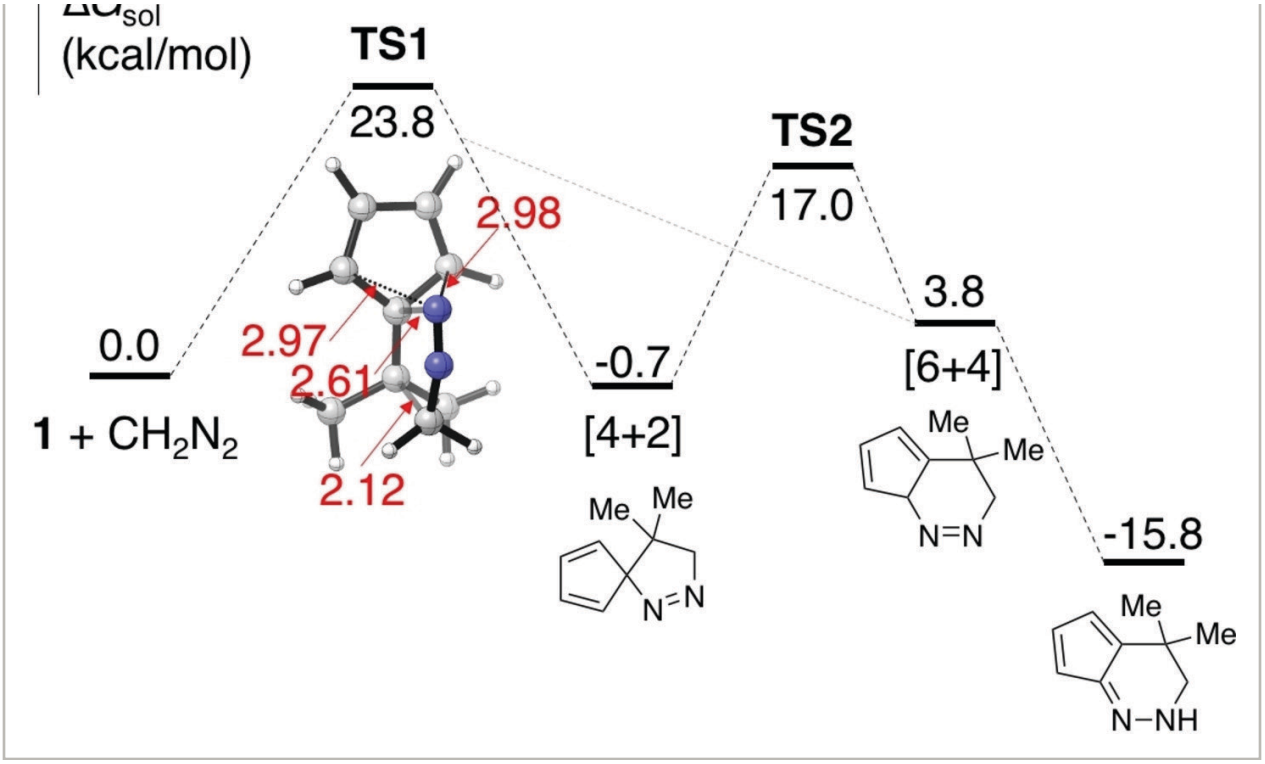

Figure 9 Open in figure viewer | PowerPoint

Free energy diagram for the diazomethane-dimethylfulvene reaction.

For Padwa's nitrile ylide-dimethylfulvene reaction, we found an ambimodal transition state. We performed molecular dynamics and predicted a 2 : 1 ratio of [6+4]: [4+2] adducts, in reasonable agreement with experimental observation of a 3 : 1 ratio. The interconversion between the [6+4] and [4+2] adducts is slow, indicating the ratio of products is kinetically or dynamically determined (Figure 10). This is the first example of an ambimodal transition state involving a Huisgen 1,3-dipole leading to two products.

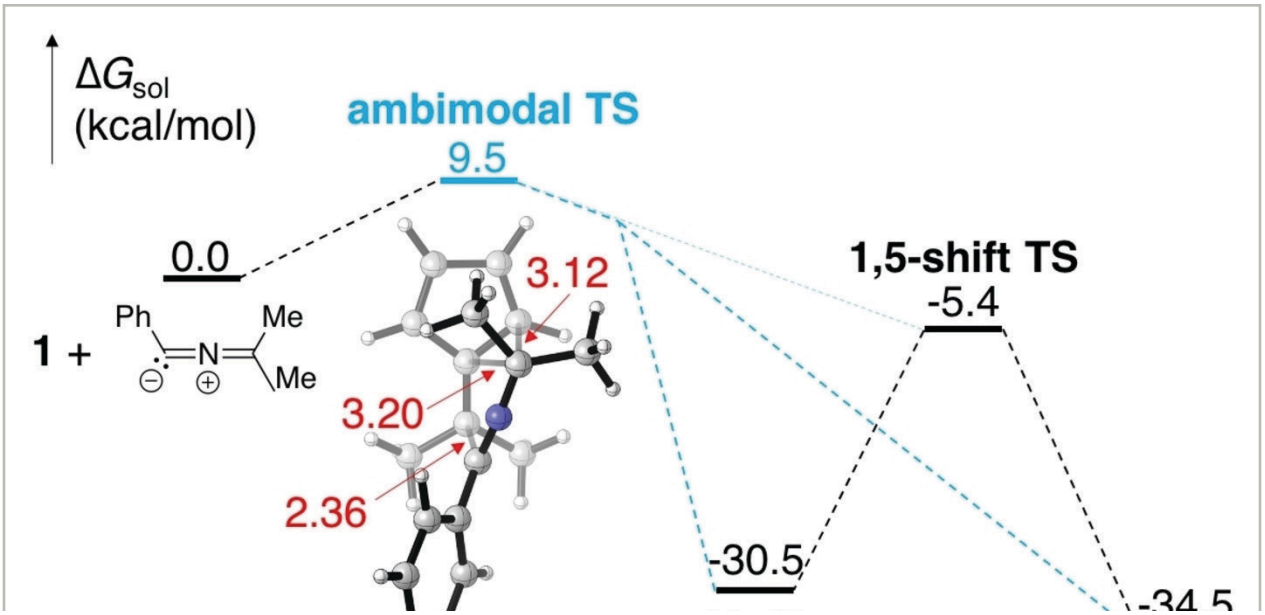

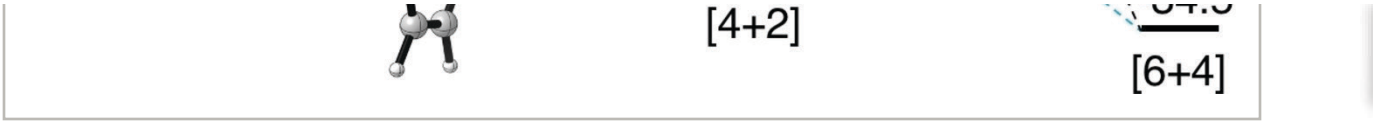

Figure 10

The free energy surface for nitrile ylide-tetramethylfulvene reaction.

2.2 Catalysis of Higher-Order Cycloadditions

In addition to the higher-order cycloadditions described in the previous section, asymmetric organocatalysis has expanded the development of novel higher-order cycloadditions with excellent selectivity and enantiocontrol.[30] Cinchona alkaloids are privileged scaffolds in catalysis,[31] and their functional diversity and adjustability have expanded the potential of such stereoselective higher-order cycloadditions.[32]

Jørgensen reported the first organocatalytic enantioselective higher-order cycloadditions using cinchona alkaloid primary amine catalysts.[33] It was demonstrated that cross- and linear-dienamine activated 2-cycloalkenones react with tropone and various heptafulvenes to provide the corresponding [6+4], [4+2], or [8+2] cycloadducts (Figure 11). It was shown that the product varied with the ring size of the cyclic enones and by changing the substitution pattern on the polyene. Before accurate quantum mechanical results were possible on such large systems, the mechanism, concerted versus stepwise, and origins of selectivity could not be easily determined. The details of mechanism can now be detailed with density functional calculations. We found that many of these reactions are not pericyclic, but instead the catalysts promote stepwise cycloadditions to give products that could have been formed by pericyclic processes.

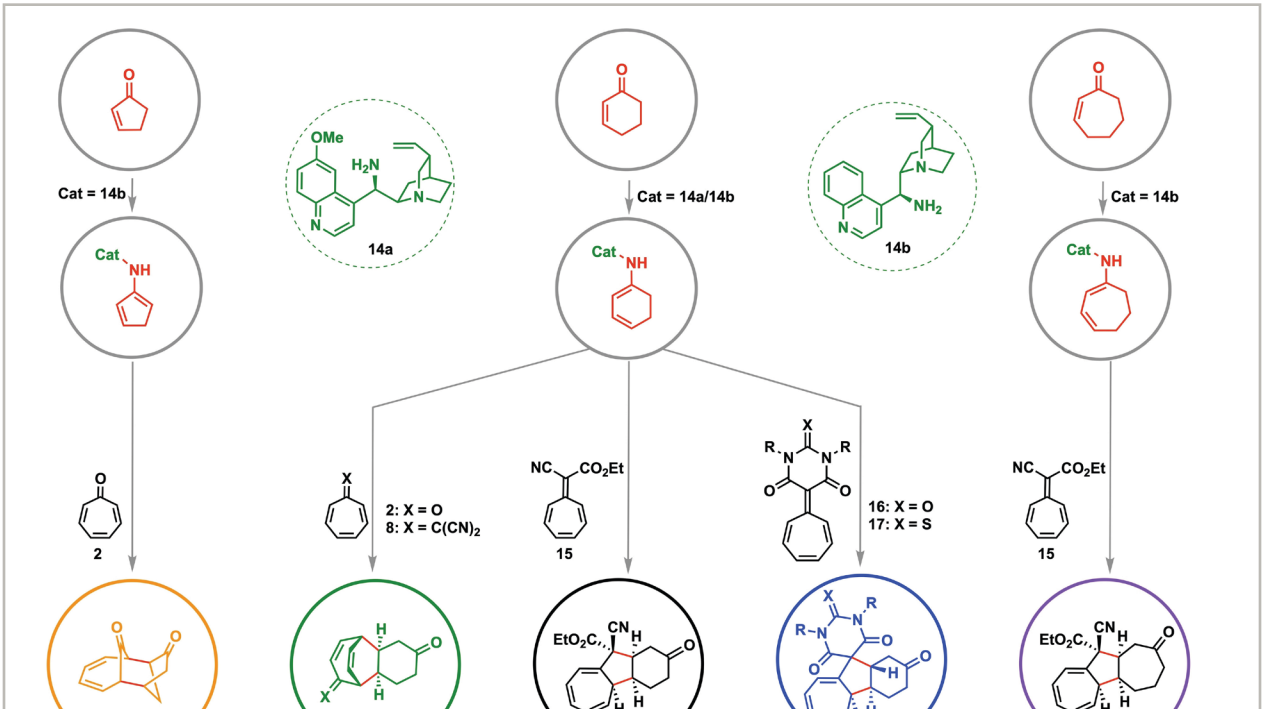

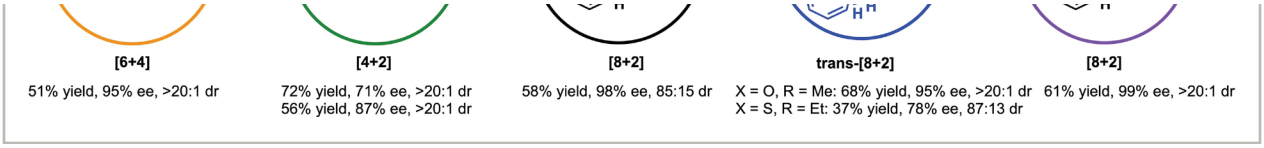

Figure 11

Open in figure viewer | PowerPoint

Organocatalytic dienamine activation of cycloalkenones and selected examples of their cycloadditions with tropone and heptafulvenes.

As shown in Figure 11, cyclopentenone and tropone **2** react, catalyzed by **14 b**, to produce exclusively the [6+4] cycloadduct in moderate to good yields, high diastereoselectivities, and good enantioselectivities. DFT calculations for cycloadditions between the dienamine intermediate(s) formed from 2-cyclopentenone and tropone, with a cinchona alkaloid primary amine catalyst, gave the results shown in Figure 12.[34]

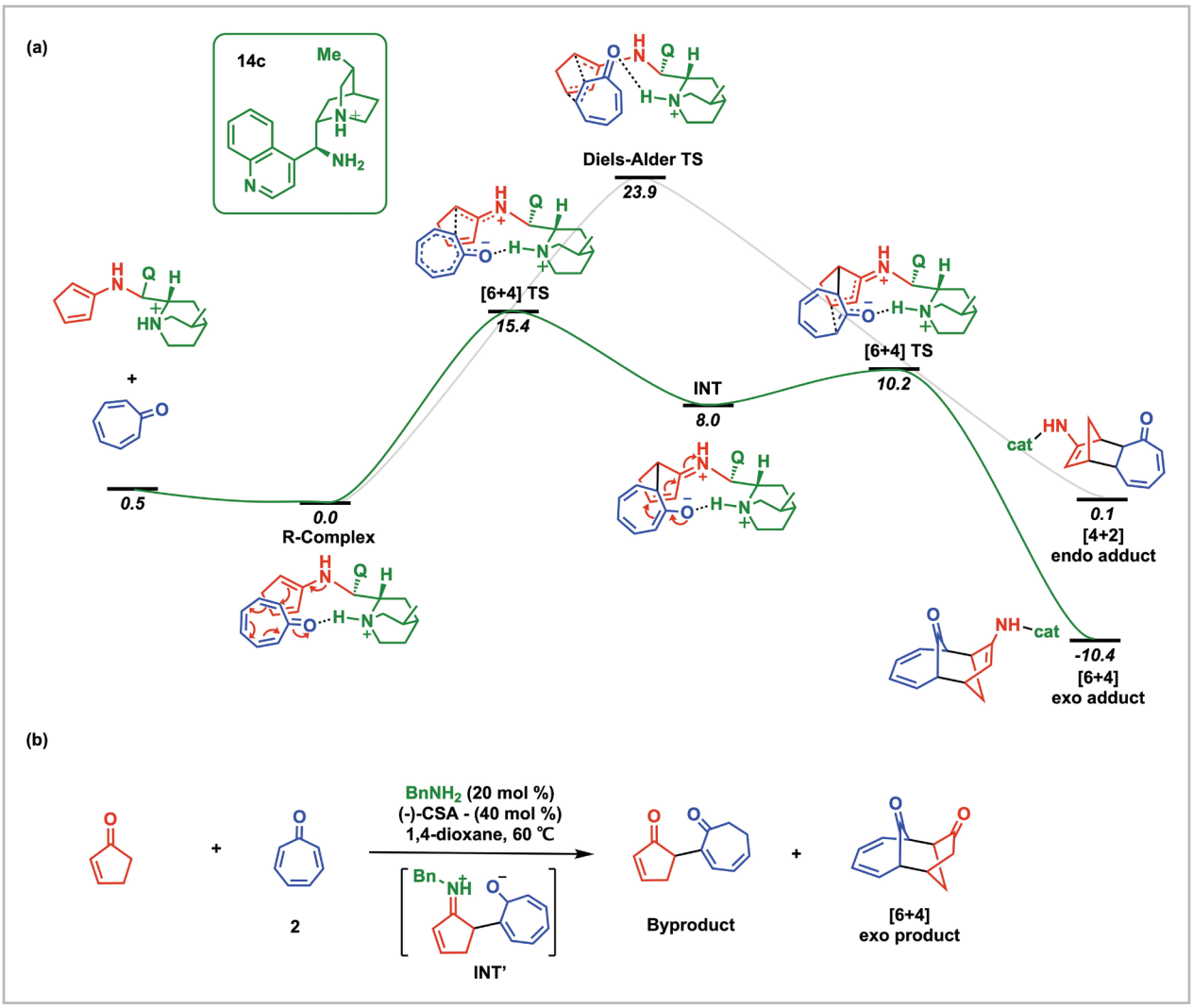

Figure 12

Open in figure viewer | PowerPoint

(a) Free energy profile of the [6+4] and [4+2] cycloadditions between tropone and

cross-dienamine intermediate. All energies are in kcal/mol. (b) Reaction Supporting a Stepwise Mechanism for the Reaction of 2-Cyclopentenone with Tropone.

The free energy profiles of [6+4] and [4+2] cycloadditions of tropone and cross-dienamine intermediate are depicted in Figure 12a. A Diels-Alder [4+2] concerted pathway is 8.5 kcal/mol higher in energy than the stepwise [6+4] pathway. The [8+2] pathway gives an unstable product (not shown). The most favorable pathway leads to the [6+4] adduct, which is consistent with experiment. The rate- and stereo- determining step is the first C–C bond formation with a total barrier of 15.4 kcal/mol, and there is a small 2 kcal/mol barrier for formation of the second bond. The stepwise mechanism is supported by formation of a non-cyclized byproduct (Figure 12b) found when benzylamine is used as organocatalyst under the standard reaction conditions. The enantioselectivity of the [6+4] cycloaddition originates from different repulsive hydrogen-hydrogen interactions that distinguish the diastereomeric transition states. The strong hydrogen-bonding interaction between the tropone oxygen and the protonated quinuclidine in the cyclic TS structure (as shown in Figure 12a) is important. This is demonstrated by the influence of the concentration of the acid additive on the yields and enantioselectivities of the reaction.

The cinchona alkaloid primary amine catalyzed cycloadditions of 2-cyclohexenone with tropone or different heptafulvenes display fundamental differences in favored reaction paths depending on the substituents present on the polyene reaction partner. As shown in Figure 11, tropone **2** and dicyanoheptafulvene **8** both react with 2-cyclohexenone catalyzed by **14 a**, to produce exclusively the [4+2] cycloadducts in moderate to good yields, high diastereoselectivities, and good enantioselectivities. In contrast, applying the same reaction conditions to cyanoester-heptafulvene leads exclusively to the formation of the corresponding [8+2] cycloadduct in good yield and high stereoselectivity. Recently,[35] the mechanisms, thermodynamics, and origins of chemo- and stereoselectivities of the organocatalytic [8+2] *vs*. [4+2] cycloadditions between 2-cyclohexenone and tropone/heptafulvenes were explained through DFT calculations, using the ωB97X–D density functional.

The cinchona alkaloid primary amine catalyst generates an ion pair catalyst with the acid additive and leads to formation of the linear dienamine and subsequently undergoes a stepwise [8+2] or [4+2]. The schematic diagram of proposed mechanism is shown in Figure 13. For the cycloaddition of 2-cyclohexanone and heptafulvenes, no hydrogen bond is formed between the tropone oxygen and the protonated quinuclidine nitrogen of the catalyst to maximize the overlap of the dienamine and tropone. Both tropone and the different heptafulvenes initially form [8+2] cycloadducts. The final product is ultimately decided by the reversibility of the [8+2] cycloaddition and the relative thermal stability of the [4+2] products (Figure 13). The stereoisomeric transition states are distinguished by the steric interactions

between the protonated catalyst and tropone/heptafulvenes. These computational studies elucidate the chemo-, regio-, and stereoselectivities of these higher-order cycloadditions and guide the experiments with heptafulvenes containing diester and barbiturate substituents. The [8+2] cycloaddition of barbiturate heptafulvene afforded products with an unprecedented trans fusion of the five- and six-membered rings as a result of its stability and a lower reversible barrier. These computational results are consistent with the excellent, but variable selectivities observed experimentally with different heptafulvene derivatives.

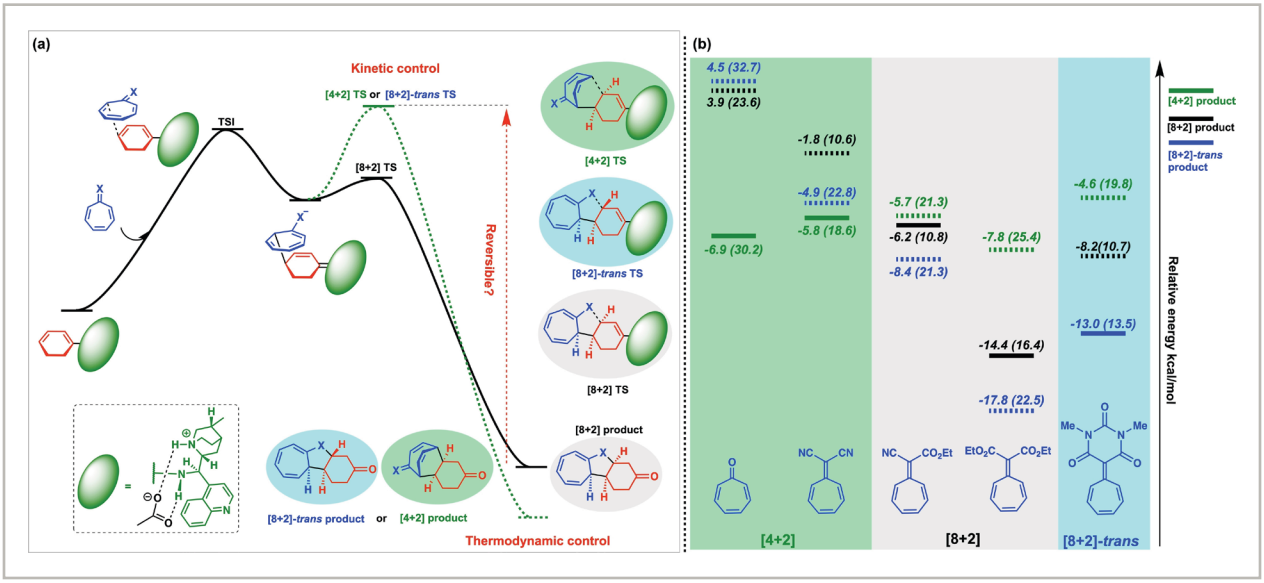

Figure 13

Open in figure viewer | PowerPoint

(a) Schematic diagram of the [8+2] and [4+2] cycloadditions between 2-cyclohexenone and heptafulvenes. (b) Gibbs free energies of [4+2] cycloadducts, [8+2] cycloadducts, and [8+2]-trans cycloadducts with respect to the respective starting materials (activation Gibbs free energies in parentheses). The experimentally observed products are marked as solid lines. All energies are in kcal/mol.

Jørgensen also reported cycloadditions of hetero-aromatic compounds via amino aza- and diazafulvenes in 2019. Our calculations also showed that these highly polar reactants undergo stepwise cycloadditions.[36] The amazing variability of these reactions could hardly be understood without the availability of modern computers and density functional theory methods. We should mention that there are a variety of ways that substituents may divert cycloadditions and other pericyclic reactions from concerted to stepwise. We should also note, as pointed out by a reviewer of this manuscript, that polarization by Lewis acid catalysts, a number of different stereoelectronic effects, aromaticity, and other factors may stabilize intermediates leading to cycloaddition products, and either influence the rates of pericyclic mechanisms or divert to non-pericyclic mechanisms.[36b]

3 Pericyclases

The pericyclases are a recently recognized family of natural enzymes that catalyze pericyclic reactions.[37] Such enzymes were hypothesized to exist for many years but remained elusive.[38-41] The first member of this enzyme family is chorismate mutase. This enzyme catalyzes the Claisen rearrangement, a [3,3]-sigmatropic pericyclic reaction in aromatic amino acid biosynthesis converting chorismate to prephenate (Figure 14). The mechanism of this Claisen rearrangement has been extensively studied; the enzyme (and antibody homologues) were cocrystallized with chair transition state analogues; extensive hydrogen-bonding interactions stabilize the transition state geometry; computational studies revealed concerted transition state geometries as well as conformational restriction leading to the greatest reduction in reaction barrier.[42-46] Computational studies played an instrumental role in characterizing the first enzymatic pericyclic reaction.

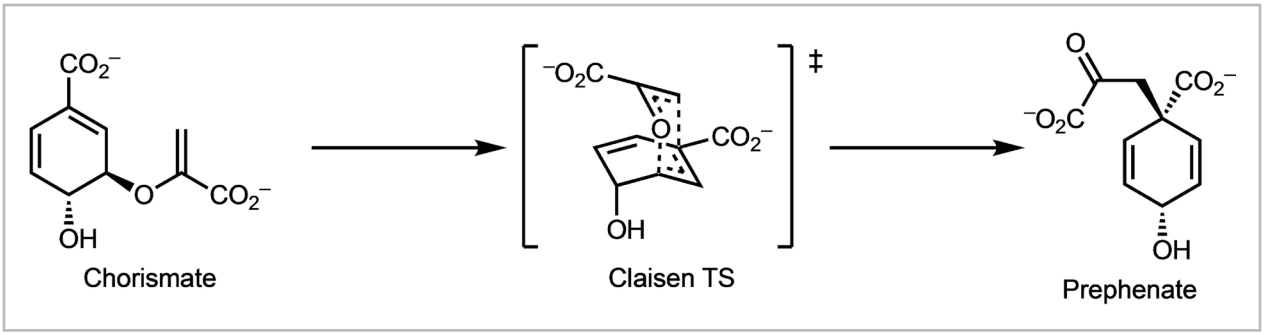

Figure 14 Open in figure viewer | PowerPoint

The first pericyclase, chorismate mutase, catalyzes this reaction.

After this work, many laboratories worked to identify natural examples of the Diels-Alder reaction. Laschat, Oikawa, and others searched for cyclohexenes and decalin motifs in natural products (Figure 15).[38, 39] Such speculation led to the discovery of multifunctional synthases, macrophomate synthase, LovB, and Sol5, that catalyze formation of the substrate and the subsequent Diels-Alder reaction (Figure 16).[47-51] However, it was difficult to characterize whether these synthases indeed *catalyze* the Diels-Alder reaction. It proved difficult to use kinetics to determine whether the enzyme catalyzes the Diels-Alder, as multiple reactions are occurring; which domain of the LovB megasynthase that is responsible for the Diels-Alder reaction could not be identified.

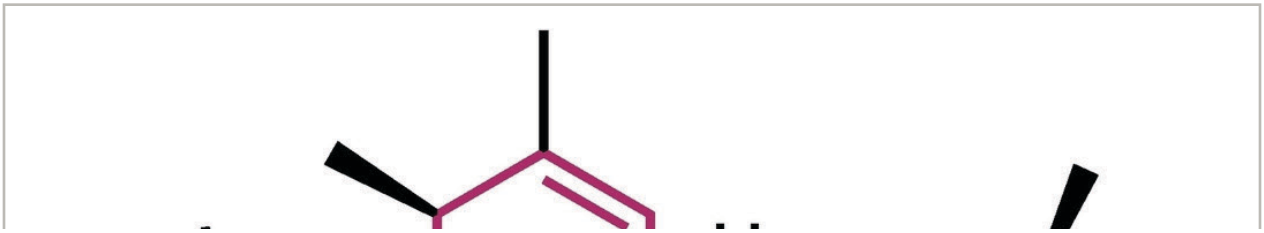

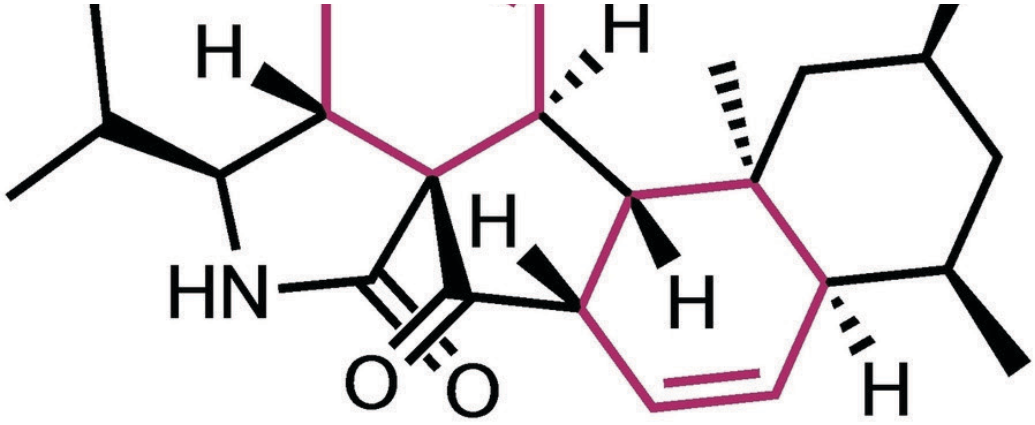

Chaetochalasin A

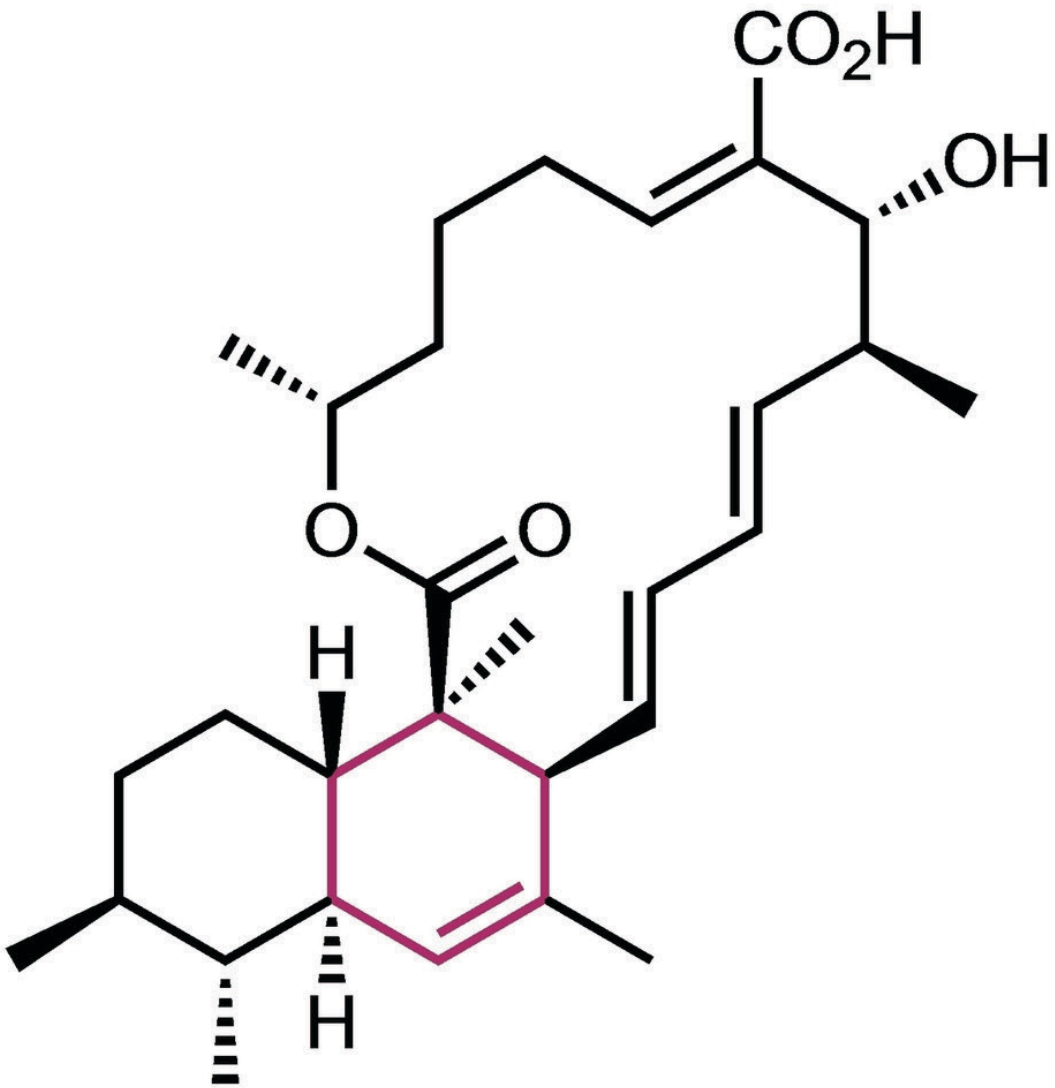

Tubelactomicin A

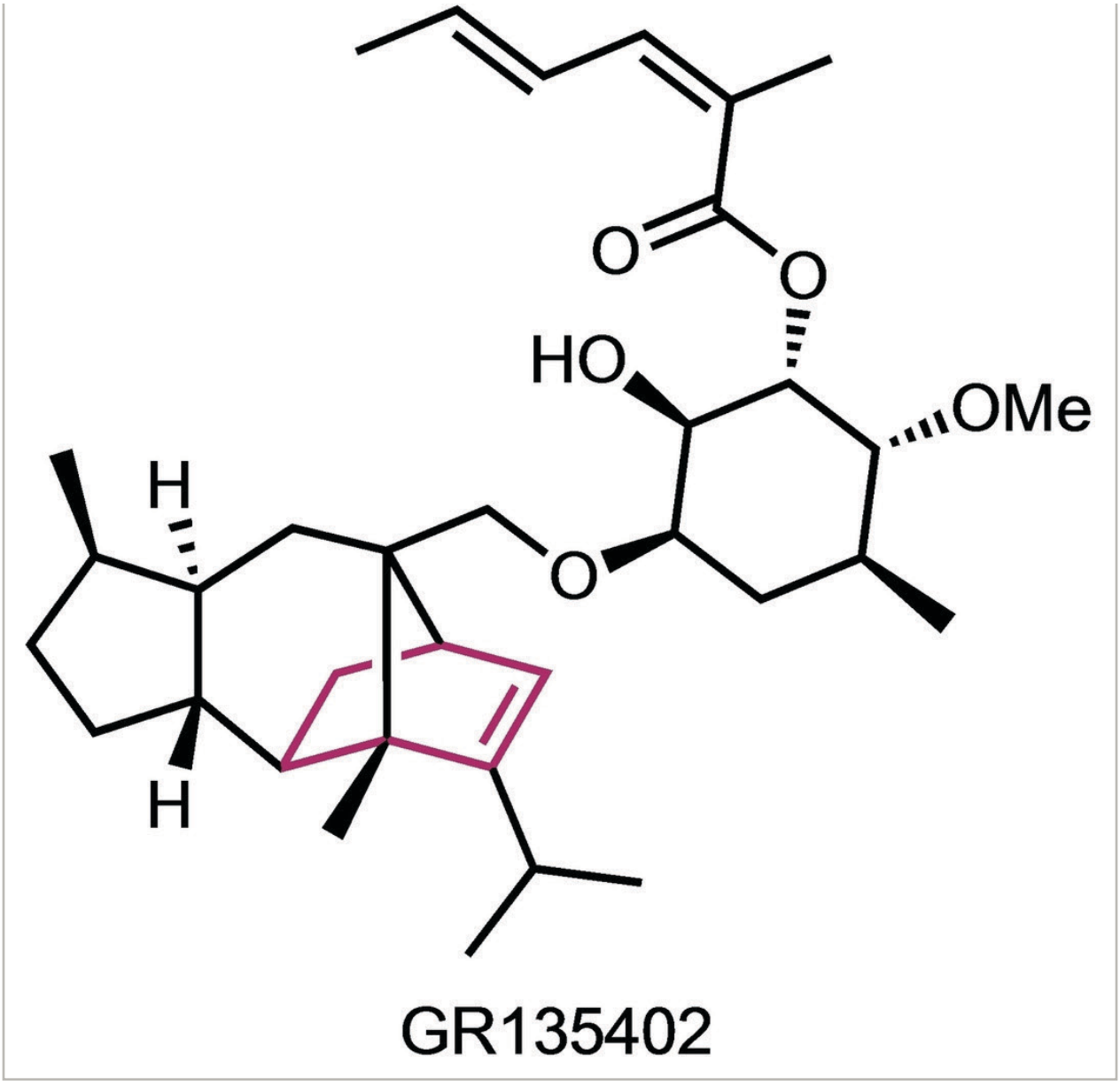

Figure 15

There must be Diels-Alderases! Cyclohexenes present in some natural products.[30, 39]

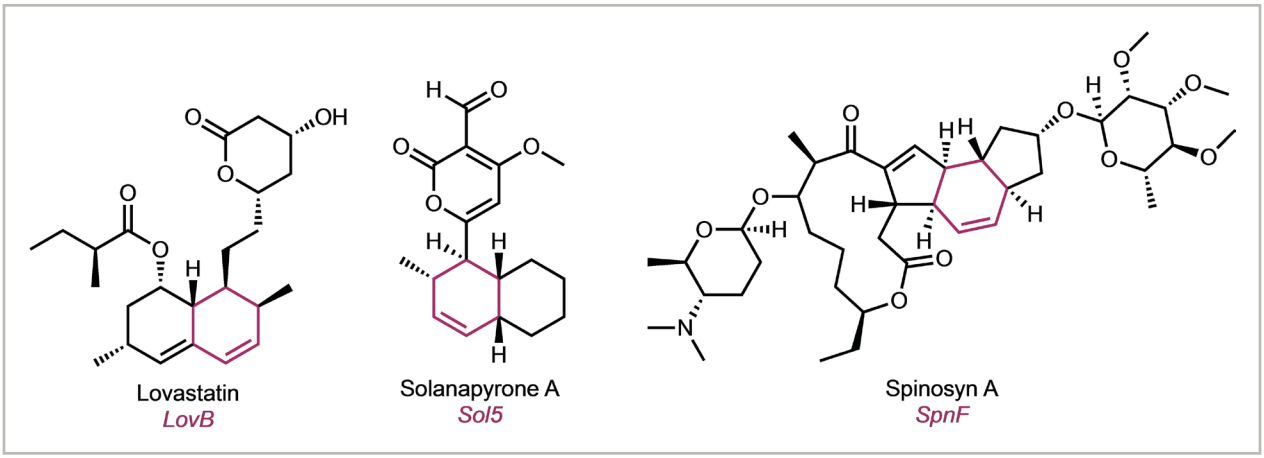

Figure 16

Structures of lovastatin, solanapyrone, spinosyn A and the enzymes that form the highlighted cyclohexenes.

It was not until 2011 that this philosophical debate on whether these enzymes were indeed catalyzing pericylic reactions was settled. At this time, the Liu laboratory at Texas discovered a monofunctional enzyme SpnF in spinosyn biosynthesis that catalyzes a transannular Diels-Alder reaction with modest (500-fold) rate acceleration (Figure 16).[52] Fascinatingly, SpnF was annotated as a *S*-adenosyl-L-methionine (SAM) dependent methyltransferase. SAM does in fact bind in the enzyme pocket but is not required for catalysis. Multiple computational studies revealed the complex nature of these transformations: this transannular Diels-Alder reaction involves an ambimodal transition state leading to both [6+4] cycloaddition and [4+2] Diels-Alder reaction.[53-57] In 2018, enzyme dynamics simulations revealed that SpnF is able to tune this ambimodal reaction away from forming the [6+4] adduct.[53] This fact paired with the thermodynamic instability of the [6+4] adduct rationalize why this product was never observed experimentally. SpnF is the first *characterized* monofunctional enzyme to catalyze a Diels-Alder reaction and first enzyme *proposed* to catalyze a higher-order cycloaddition.

Around this time, significant advances in genome sequencing and gene cluster identification facilitated discoveries of bacterial Diels-Alder reactions catalyzed by beta-barrel enzymes PyrE3 and PyrI4 in pyrroindomycin bionsynthesis and characterization of homologues VstJ and AbyU.[58, 59] Bioinformatics also revealed fungal lipocalin-like enzymes that catalyze Diels-Alder reactions of tetramic acids and related pyrrolinones; i. e. CghA in Sch210972 biosynthesis, Fsa2 in equisetin biosynthesis, MycB in myceliothermophin biosynthesis, and PvhB in varicidin biosynthesis (Figure 17).[60-64]

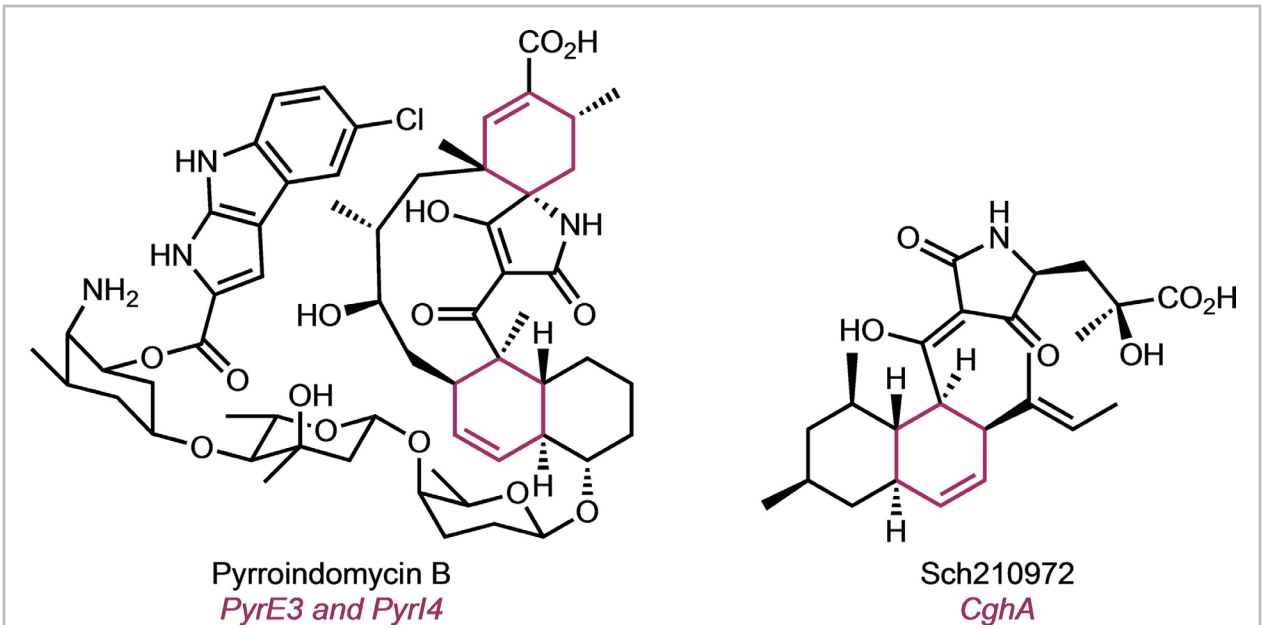

Figure 17

Exemplary tetramic acid natural products pyrroindomycin B and Sch210972 and the enzymes that form the highlighted cyclohexenes.

We turn to recent experimental and computational collaborations that characterize ambimodal pericyclases, intermolecular pericyclases, and pericyclases that catalyze other pericyclic reactions.

3.1 Ambimodal Pericyclases

There are three prominent examples of natural ambimodal pericyclases; LepI in leporin biosynthesis,[65, 66] IccD in ilicicolin biosynthesis,[67] and StmD (and NgnD) in streptoseomycin biosynthesis.[68]

The leporins are tricyclic isochromene pyridone alkaloid natural products. Biosynthesis requires a SAM-dependent *O*-methyl transferase-like enzyme LepI that catalyzes, instead of the canonical *O*-methylation reaction, a two-step cascade: a stereoselective dehydration followed by a concomitant ambimodal [4+2] hetero-Diels-Alder/[4+2] Diels-Alder cycloadditions (Figure 18a).[65] Quasi-classical reaction dynamics simulations of a highly simplified model system revealed that both the hetero-Diels-Alder and Diels-Alder adducts are formed in a 17 : 83 ratio. *In vitro* experiments showed that LepI is also able to catalyze the retro Claisen rearrangement of the [4+2] Diels-Alder adduct into the [4+2] hetero-Diels-Alder adduct, leporin C. Fascinatingly, SAM is required for these pericyclic reactions to occur, despite being more than 5 Å away from the substrate in the active site.[66] SAM seems to plays a crucial structural role in configuring the LepI active site. We propose (and are currently investigating) that SAM also acts as an electrostatic catalyst to stabilize the transition state by modifying the dipole in the enzyme active site. Examples of electrostatic catalysis have been demonstrated by Warshel, Wilcox, Boxer, Shaik, Coote, and T. Head-Gordon. Calculations revealed that these reactions are highly asynchronous and ambimodal.

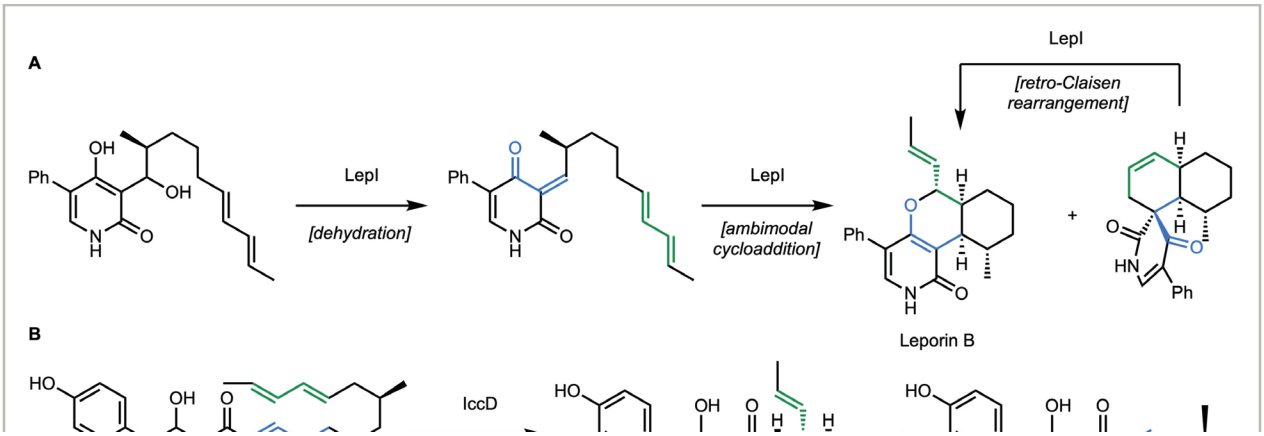

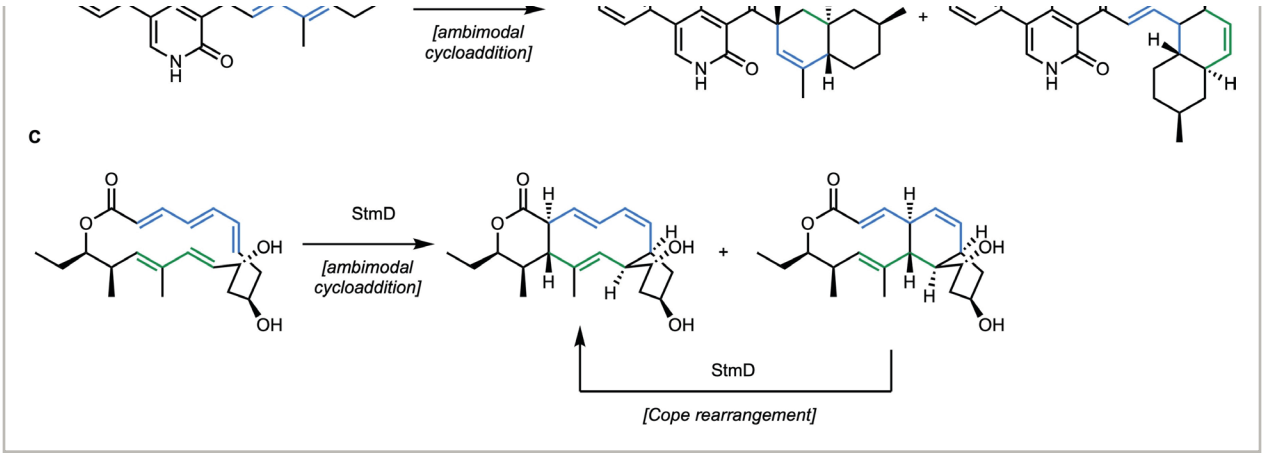

Figure 18

Open in figure viewer | PowerPoint

Ambimodal reactions in biosynthesis. (A) Leporin biosynthesis involves an ambimodal cycloaddition forming hetero-Diels-Alder and Diels-Alder products catalyzed by LepI. (B) Illicicolin biosynthesis involves ambimodal normal and inverse electron demand Diels-Alder reactions catalyzed by IccD. (C) Streptoseomycin biosynthesis involves an ambimodal [6+4] cycloaddition/[4+2] Diels-Alder reaction catalyzed by StmD.

In 2019, ambimodal normal and inverse electron demand Diels-Alder reactions were discovered in ilicicolin biosynthesis (Figure 18b).[67] Ilicicolin H and I are pyridone alkaloid natural products that features a decalin motif. The epimer of ilicicolin H named *epi*-8-ilicicolin H can be interconverted with ilicicolin I via a Cope rearrangement. The acyclic *bis*-diene substrate binds to the monofunctional *C*-methyl transferase-like pericyclase IccD active site and reacts via an ambimodal [4+2]/[4+2] Diels-Alder transition state to form *epi*-8-ilicicolin H and a minor percentage of iliciolin I. The pericyclase IccD accelerates the ambimodal cycloaddition by >10^6-fold. Though there is no crystallographic information on the structure of IccD, we were able to reproduce experimental results for enzymatic reaction with quasi-classical reaction dynamics simulations by modifying the protonation state of the pyridone ring. In the non-enzymatic reaction occurring in buffered solution, it is likely that the substrate 4-position is deprotonated. Sequence data of IccD indicates there to be a highly hydrophobic active site. With this in mind, it is possible to envision a proton transfer upon entry to the active site to afford a neutral substrate protonated at the 4-position to coordinate to the enzyme. Reaction dynamics simulations in the neutral state reproduce the experimental enzymatic results; a ratio of 99 : 1 of *epi-8*-ilicicolin H and ilicicolin I are formed in dynamics simulations and in experiment. Further studies of this system are warranted upon crystallization this enzyme.

The biosynthesis of streptoseomycin was characterized in 2019. Streptoseomycin is a macrolactone natural product that is related to the spinosyn natural products (*vide supra*). In this case, streptoseomycin is formed by an ambimodal [6+4] cycloaddition/[4+2] Diels-Alder

reaction (Figure 18c).[68] This ambimodal cycloaddition is catalyzed by the monofunctional enzymes StmD and NgnD. However, unlike spinosyn biosynthesis, in this case the [6+4] adduct is stable and able to be isolated and characterized. This fact verifies that our and others' computational simulations predicting such reactions to be ambimodal are rooted in reality in both streptoseomycin and spinosyn biosynthesis. The enzymes StmD and NgnD catalyze the ambimodal [6+4] cycloaddition/[4+2] Diels-Alder reaction, and the [4+2] adduct can be converted by a Cope rearrangement to more stable [6+4] adduct that is enzymatically transformed to streptoseomycin.

3.2 Intermolecular Pericyclases

Intermolecular Diels-Alder reactions are crucial in synthesis, with classic examples in Woodward's synthesis of reserpine or Stork's synthesis of germine. Such intermolecular Diels-Alder reactions escaped characterization in nature until 2019. Previously these reactions had been proposed by Cox and coworkers in xenovulvene biosynthesis, but the enzyme responsible for the intermolecular hetero-Diels-Alder reaction remained elusive.[69] A collaboration between the Hu and Houk laboratories led to discovery of a related enzyme EupF that catalyzes the formation of neosetophomone B, a tropolonic sesquiterpene related to xenovulvene.[70] This enzyme EupF catalyzes a dehydration to form a quinone methide that then undergoes a barrierless, concerted hetero-Diels-Alder reaction to selectively form neosetophomone B. Interestingly, the mechanism and enzyme responsible for the second addition of tropolone to form ditropolonic sesquiterpenes eupenifeldin and pycnidione are still uncharacterized. ((Figure 19))

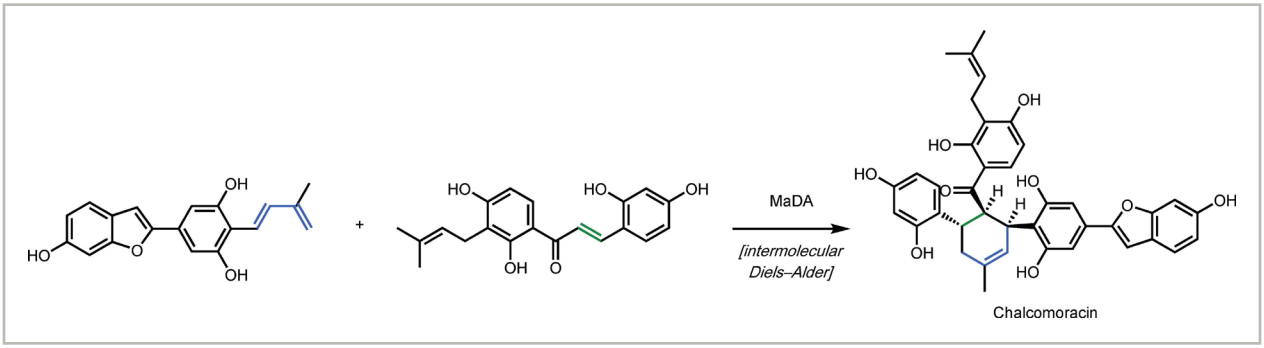

Figure 19 Open in figure viewer | PowerPoint

The intermolecular Diels-Alder reaction forming chalcomoracin catalyzed by MaDA.

Building off this work, the laboratories of Lei, Dai, Huang, and Houk discovered pericyclases that catalyze monofunctional intermolecular Diels-Alder reactions in plant natural product biosynthesis. Two homologous (61 %) flavin adenine dinucleotide (FAD)-dependent enzymes named MaMO and MaDA were discovered.[71] The enzyme MaMO oxidizes the prenyl unit of

moracin C to form a terminal reactive diene. The oxidized product and morachalcone A, which features an activated α,β-unsaturated ketone, migrate and bind to the active site of MaDA and undergo a Diels-Alder reaction to form the central cyclohexene of chalcomoracin. Currently, we are collaborating to rationalize the *endo* and *exo* selectivity in these Diels-Alder reactions. These studies have led to the discovery and characterization of homologous enzymes that catalyze the *exo*-Diels-Alder reaction exclusively.

3.3 Pericyclases that Catalyze other Pericyclic Reactions

Since 2020, pericyclic reactions other than cycloadditions have been discovered in nature. Alder-ene reactions have been characterized in pyridoxatin biosynthesis.[72] This key reaction forms the vinyl cyclohexyl core of pyridoxatin and gives rise to the atropisomeric nature of this natural product. The enzyme responsible for this transformation is predicted to be a SAM-dependent *O*-methyltransferase but instead catalyzes a two-step cascade: a stereoselective dehydration to form a (*Z*)-quinone methide that then undergoes an Alder-ene reaction (Figure 20). This reaction sequence is related to the previously described example, LepI. However, PdxI is different by (1) not requiring SAM for catalysis, (2) catalyzing a dehydration to form a (*Z*)-quinone methide, versus (*E*)-quinone methide, and (3) catalyzing the more difficult pericyclic reaction, an Alder-ene reaction versus hetero-Diels-Alder. In the binding pocket of PdxI, the canonical SAM binding residues are mutated to bulky hydrophobic residues that drastically decrease the size of the active site. A cocrystal structure with a substrate analogue revealed that the quinone methide formed from dehydration is in the (*Z*) geometry. From this (*Z*)-quinone methide, either a hetero-Diels-Alder or Alder-ene reaction are possible. Energetically, the Alder-ene reaction is more difficult due to product instability relative to the hetero-Diels-Alder. However, PdxI is able to alter the intrinsic periselectivity by hydrogen bond catalysis. Classical molecular dynamics simulations of the reactive (*Z*)-quinone methide revealed a key lysine residue that hydrogen bonds to the 4-position of the pyridone. Quantum mechanical calculations including a model of this residue revealed that hydrogen bonding reverses the periselectivity and favors Alder-ene formation. Removal of the lysine residue hydrogen bond by mutating the adjacent residue reverses periselectivity, and a hetero-Diels-Alder product is observed which corresponds to the natural product asperpyridone scaffold. Based on this result, a second mutation of the threonine residue was predicted in order to have the hetero-Diels-Alder occur at adjacent 2-position hetero-diene. A large scale reaction with the threonine mutant indeed formed a new 4-pyridone scaffold that has yet to be isolated in nature. In total, these studies characterized the first Alder-ene reaction in biology and found single point mutations that modulate the natural periselectivity. These examples also emphasize the crucial role of computations in exploring and elucidating mechanisms of enzyme-catalyzed pericyclic reactions.

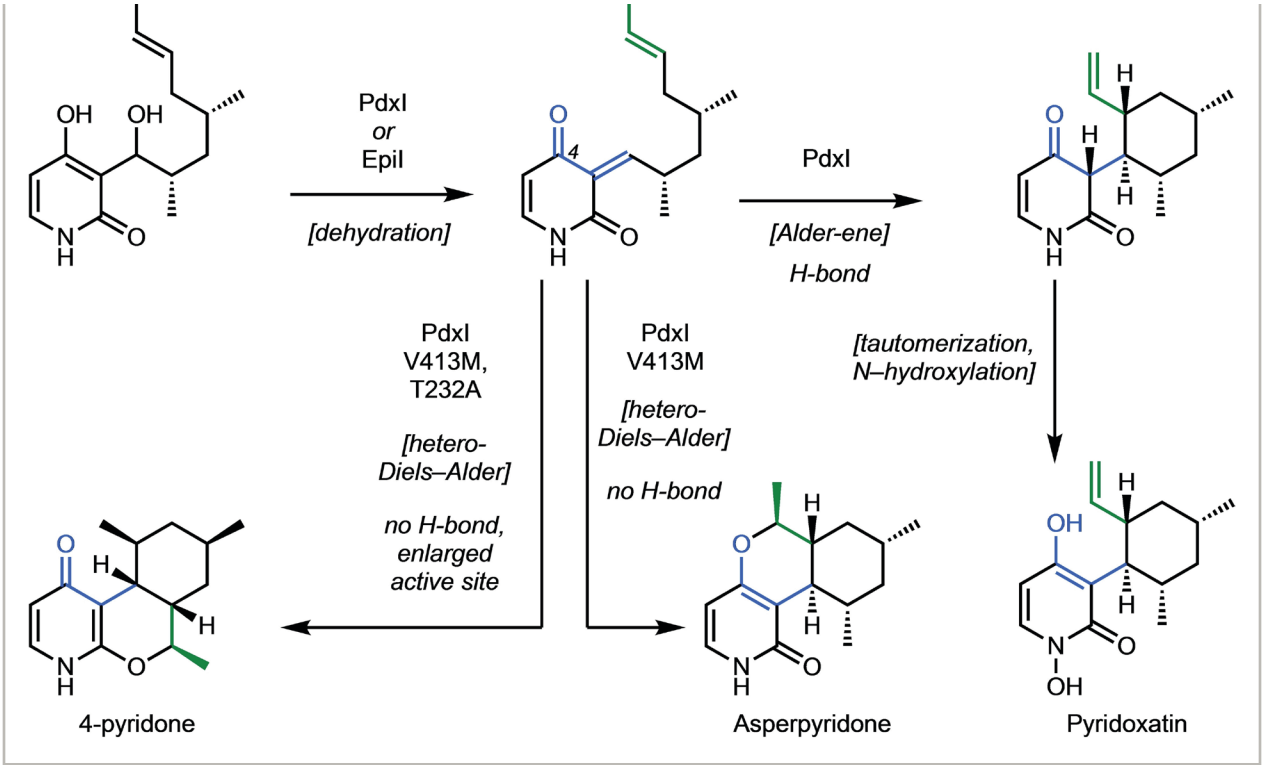

Figure 20 Open in figure viewer | PowerPoint

Enzymatic Alder-ene reaction catalyzed by PdxI to form natural product pyridoxatin and mutational studies to form hetero-Diels-Alder adducts.

We believe that these discoveries of enzymatic Alder-ene reactions will stimulate the field to investigate and characterize other pericyclic reactions in natural systems. Previous work by Hilvert and coworkers proposed a retro-oxa-ene reaction in bacterial sideophore biosynthesis;[73] Nay and coworkers proposed AuaG-catalyzed [2,3]-Wittig rearrangements and Claisen rearrangements in aurachin B biosynthesis;[74] Shipman and coworkers proposed precorrin-8x methyl mutase CobH to catalyze a [1,5]-sigmatropic rearrangement.[75] The Sherman and Liu laboratories have reported Cope rearrangements in hapalindole, fischerindole, ambiguine, and welwitindole biosynthesis.[76, 77] Our recent computational work revealed a dissociative step-wise mechanism for these Cope rearrangements.[76] Many more pericyclases are clearly lurking in nature's synthetic machinery, waiting to be discovered.

4 Conclusion and Prospects for the Future

This article has described how mechanistic understanding about pericyclic reactions, particularly higher-order cycloadditions, has advanced due to the enormous developments of computer power and methods in the last half-century. We believe that current quantum mechanical accuracy is sufficient to give very precise descriptions of mechanisms of gas phase reactions that do not involve formations of ions from neutrals. Our predictions of gas phase pericyclic reactions are likely very accurate.

Of course, most reactions are carried out in solution, and the computation of reliable high-accuracy energetics in solution, or in enzymes, is not routine, and future developments in methods and computers will open up new vistas in the understanding of reactions in solution and in enzymes. Pericyclic reactions generally do not involve significant charge development, and solvation energies are not so important in relatively high accuracy results for solutions and enzymes are possible for this subset of organic reactions.

More generally, the certain increase in computational power in the next few decades will make it possible to develop accurate methods for studies of reaction mechanisms in solution, including reactions in which ions and ion pairs are generated. The kind of geometrical and temporal resolution that we demonstrate here will become possible for all types of reactions in solution and in enzymes.

Acknowledgements

We are grateful to the National Science Foundation of the USA (CHE-1764328 and CHE-CLP-1806581) for financial support of the Houk group research. We have had many fruitful collaborations with experimental groups all over the world and are especially grateful to the discussions with Professors Yi Tang of UCLA and Karl Anker Jørgensen of Aarhus University.

References

1 C. K. Ingold, *Structure and Mechanism in Organic Chemistry*, Cornell University Press, Ithaca, NY, 1953.
Google Scholar | Get it at UC

2 S. Winstein, D. S. Trifan, *J. Am. Chem. Soc.* 1949, **71**(8), 2953– 2954.
Crossref | CAS | Web of Science® | Google Scholar | Get it at UC

3 R. B. Woodward, T. J. Katz, *Tetrahedron* 1959, **5**, 70– 89.
Crossref | CAS | Web of Science® | Google Scholar | Get it at UC

4

4a K. Fukui, T. Yonezawa, H. Shingu, *J. Chem. Phys.* 1952, **20**, 722– 725;
Crossref | CAS | Web of Science® | Google Scholar | Get it at UC

4b I. Fleming, *Frontier Orbitals and Organic Chemical Reactions*, Wiley, London, 1968;

Google Scholar | Get it at UC

4c I. Fleming, *Molecular Orbitals and Organic Chemical Reactions*, John Wiley & Sons, Ltd., Chichester, 2009.
Wiley Online Library | Google Scholar | Get it at UC

5 R. B. Woodward, R. Hoffmann, *The Conservation of Orbital Symmetry*, Weinheim, BRD: Verlag Chemie GmbH (BRD) and Academic Press (USA), 1971, pp. 1– 178.
Crossref | Google Scholar | Get it at UC

6 K. N. Houk, J. Gonzalez, Y. Li, *Acc. Chem. Res.* 1995, **28**, 81– 90.
Crossref | CAS | Web of Science® | Google Scholar | Get it at UC

7 K. N. Houk, F. Liu, *Acc. Chem. Res.* 2017, **50**, 539– 543.
Crossref | CAS | PubMed | Web of Science® | Google Scholar | Get it at UC

8 D. McLeod, M. K. Thogersen, N. I. Jessen, K. A. Jorgensen, C. S. Jamieson, X. S. Xue, K. N. Houk, F. Liu, R. Hoffmann, *Acc. Chem. Res.* 2019, **52**, 3488– 3501.
Crossref | CAS | PubMed | Web of Science® | Google Scholar | Get it at UC

9 R. Hoffmann, R. B. Woodward, *J. Am. Chem. Soc.* 1965, **87**(9), 2046.
Crossref | CAS | Web of Science® | Google Scholar | Get it at UC

10

10a K. N. Houk, R. B. Woodward, *J. Am. Chem. Soc.* 1970, **92**, 4143– 4145;
Crossref | CAS | Web of Science® | Google Scholar | Get it at UC

10b K. N. Houk, R. B. Woodward, *J. Am. Chem. Soc.* 1970, **92**, 4145– 4147;
Crossref | CAS | Web of Science® | Google Scholar | Get it at UC

10c K. N. Houk, L. J. Luskus, N. S. Bhacca, *J. Am. Chem. Soc.* 1970, **92**, 6392– 6394.
Crossref | CAS | Web of Science® | Google Scholar | Get it at UC

11 K. N. Houk, L. J. Luskus, N. S. Bhacca, *J. Am. Chem. Soc.* 1970, **92**, 6392– 6394. [same as 10c].
Crossref | CAS | Web of Science® | Google Scholar | Get it at UC

12

12a M. N. Paddon-Row, R. N. Warrener, *Tetrahedron Lett.* 1974, **15**, 3797– 3800;
Crossref | Google Scholar | Get it at UC

12b M. N. Paddon-Row, *Aust. J. Chem.* 1974, **27**, 299– 313.
Crossref | CAS | Web of Science® | Google Scholar | Get it at UC

13 P. Yu, T. Q. Chen, Z. Yang, C. Q. He, A. Patel, Y.-h. Lam, C.-Y. Liu, K. N. Houk, *J. Am. Chem. Soc.* 2017, **139**, 8251– 8258.
Crossref | CAS | PubMed | Web of Science® | Google Scholar | Get it at UC

14 H. V. Pham, K. N. Houk, *J. Org. Chem.* 2014, **79**, 8968– 8976.
Crossref | CAS | PubMed | Web of Science® | Google Scholar | Get it at UC

15 P. Caramella, P. Quadrelli, L. Toma, *J. Am. Chem. Soc.* 2002, **124**, 1130– 1131.
Crossref | CAS | PubMed | Web of Science® | Google Scholar | Get it at UC

16

16a D. H. Ess, S. E. Wheeler, R. G. Iafe, L. Xu, N. Celebi-Olcum, K. N. Houk, *Angew. Chem. Int. Ed.* 2008, **47**, 7592– 7601;
Wiley Online Library | CAS | PubMed | Web of Science® | Google Scholar | Get it at UC
Angew. Chem. 2008, **120**, 7704– 7713;
Wiley Online Library | Google Scholar | Get it at UC

16b S. R. Hare, D. J. Tantillo, *Pure Appl. Chem.* 2017, **89**, 679– 698.
Crossref | CAS | Web of Science® | Google Scholar | Get it at UC

17 K. Black, P. Liu, L. Xu, C. Doubleday, K. N. Houk, *Proc. Natl. Acad. Sci. USA* 2012, **109**, 12860– 12865.
Crossref | CAS | PubMed | Web of Science® | Google Scholar | Get it at UC

18 P. Yu, T. Q. Chen, Z. Yang, C. Q. He, A. Patel, Y.-h. Lam, C.-Y. Liu, K. N. Houk, *J. Am. Chem. Soc.* 2017, **139**, 8251– 8258. [*same* as 13].
Crossref | CAS | PubMed | Web of Science® | Google Scholar | Get it at UC

19 X.-S. Xue, C. S. Jamieson, M. Garcia-Borràs, X. Dong, Z. Yang, K. N. Houk, *J. Am. Chem. Soc.* 2019,

141, 1217– 1221.
Crossref | CAS | PubMed | Web of Science® | Google Scholar | Get it at UC

20 C. Y. Liu, S. T. Ding, *J. Org. Chem.* 1992, **57**, 4539– 4544.
Crossref | CAS | Web of Science® | Google Scholar | Get it at UC

21 A. Martin-Somer, X.-S. Xue, C. S. Jamieson, Y. Zou, K. N. Houk, Manuscript in preparation.
Google Scholar | Get it at UC

22 C. S. Jamieson, A. Sengupta, K. N. Houk, *J. Am. Chem. Soc.* 2021, **143**, 3918– 3926.
Crossref | CAS | PubMed | Web of Science® | Google Scholar | Get it at UC

23 R. Huisgen, *Proc. Chem. Soc. London* 1961, 357– 396.
Web of Science® | Google Scholar | Get it at UC

24

24a R. Huisgen, *Angew. Chem. Int. Ed. Engl.* 1968, **7**, 321– 328;
Wiley Online Library | CAS | Web of Science® | Google Scholar | Get it at UC

24b R. Huisgen, *Angew. Chem.* 1968, **80**, 329– 337;
Wiley Online Library | Google Scholar | Get it at UC
Angew. Chem. Int. Ed. 1968, **7**, 321– 328.
Wiley Online Library | CAS | Web of Science® | Google Scholar | Get it at UC

25

25a R. B. Woodward, R. Hoffmann, *Angew. Chem. Int. Ed. Engl.* 1969, **8**, 781– 853;
Wiley Online Library | CAS | Web of Science® | Google Scholar | Get it at UC

25b R. B. Woodward, R. Hoffmann, *Angew. Chem.* 1969, **81**, 797– 869;
Wiley Online Library | Google Scholar | Get it at UC
Angew. Chem. Int. Ed. 1969, **8**, 781– 853.
Wiley Online Library | CAS | Web of Science® | Google Scholar | Get it at UC

26 K. Alder, R. Braden, F. H. Flock, *Chem. Ber.* 1961, **94**, 456– 479.
Wiley Online Library | CAS | Web of Science® | Google Scholar | Get it at UC

27 K. N. Houk, L. J. Luskus, *Tetrahedron Lett.* 1970, **11**, 4029– 4031.
Crossref | Google Scholar | Get it at UC

28 A. Padwa, F. Nobs, *Tetrahedron Lett.* 1978, **19**, 93– 96.
Crossref | Google Scholar | Get it at UC

29 F. Liu, Y. Chen, K. N. Houk, *Angew. Chem. Int. Ed.* 2020, **59**, 12412– 12416;
Wiley Online Library | CAS | PubMed | Web of Science® | Google Scholar | Get it at UC
Angew. Chem. 2020, **132**, 12512– 12516.
Wiley Online Library | Google Scholar | Get it at UC

30

30a I. Kallweit, C. Schneider, *Org. Lett.* 2019, **21**, 519– 523;
Crossref | CAS | PubMed | Web of Science® | Google Scholar | Get it at UC

30b K. Balanna, K. Madica, S. Mukherjee, A. Ghosh, T. Poisson, T. Besset, G. Jindal, A. T. Biju, *Chem. Eur. J.* 2020, 26, 818– 822;
Web of Science® | Google Scholar | Get it at UC

30c G. Bertuzzi, M. K. Thøgersen, M. Giardinetti, A. Vidal-Albalat, A. Simon, K. N. Houk, K. A. Jørgensen, *J. Am. Chem. Soc.* 2019, **141**, 3288– 3297;
Crossref | CAS | PubMed | Web of Science® | Google Scholar | Get it at UC

30d D. McLeod, A. Cherubini-Celli, N. Sivasothirajah, C. H. McCulley, M. L. Christensen, K. A. Jørgensen, *Chem. Eur. J.* 2020, **26**, 11417– 11422;
Wiley Online Library | CAS | PubMed | Web of Science® | Google Scholar | Get it at UC

30e B. S. Donslund, A. Monleón, T. A. Palazzo, M. L. Christensen, A. Dahlgaard, J. D. Erickson, K. A. Jørgensen, *Angew. Chem. Int. Ed.* 2018, **57**, 1246– 1250;
Wiley Online Library | CAS | PubMed | Web of Science® | Google Scholar | Get it at UC
Angew. Chem. 2018, **130**, 1260– 1264;
Wiley Online Library | Google Scholar | Get it at UC

30f Z. Gao, C. Wang, L. Zhou, C. Yuan, Y. Xiao, H. Guo, *Org. Lett.* 2018, **20**, 4302– 4305;
Crossref | CAS | PubMed | Web of Science® | Google Scholar | Get it at UC

30g S. Wang, C. Rodríguez-Escrich, M. Finachini, F. Maseras, M. A. Pericàs, *Org. Lett.* 2019, **21**, 3187–

3192;
Crossref | CAS | PubMed | Web of Science® | Google Scholar | Get it at UC

30h C. He, Z. Li, H. Zhou, J. Xu, *Org. Lett.* 2019, **21**, 8022– 8026;
Crossref | CAS | PubMed | Web of Science® | Google Scholar | Get it at UC

30i S. Frankowski, A. Skrzyńska, L. Albrecht, *Chem. Commun.* 2019, **55**, 11675– 11678;
Crossref | CAS | PubMed | Web of Science® | Google Scholar | Get it at UC

30j R. Manzano, A. Romaniega, L. Prieto, E. Díaz, E. Reyes, U. Uria, U. Carrillo, J. L. Vicario, *Org. Lett.* 2020, **22**, 4721– 4725;
Crossref | CAS | PubMed | Web of Science® | Google Scholar | Get it at UC

30k B. S. Donslund, N. I. Jessen, G. Bertuzzi, M. Giardinetti, T. A. Palazzo, M. L. Christensen, K. A. Jørgensen, *Angew. Chem. Int. Ed.* 2018, **57**, 13182– 13186;
Wiley Online Library | CAS | PubMed | Web of Science® | Google Scholar | Get it at UC
Angew. Chem. 2018, **130**, 13366– 13370;
Wiley Online Library | Google Scholar | Get it at UC

30l D. McLeod, M. K. Thøgersen, N. I. Jessen, K. A. Jørgensen, C. S. Jamieson, X.-S. Xue, K. N. Houk, F. Liu, R. Hoffmann, *Acc. Chem. Res.* 2019, **52**, 3488– 3501;
Crossref | CAS | PubMed | Web of Science® | Google Scholar | Get it at UC

30m G. Bertuzzi, D. McLeod, L.-M. Mohr, K. A. Jørgensen, *Chem. Eur. J.* 2020, **26**, 15491– 15496 ;
Wiley Online Library | CAS | PubMed | Web of Science® | Google Scholar | Get it at UC

30n S. Wang, C. Rodríguez-Escrich, M. A. Pericàs, *Angew. Chem. Int. Ed.* 2017, **56**, 15068– 15072;
Wiley Online Library | CAS | PubMed | Web of Science® | Google Scholar | Get it at UC
Angew. Chem. 2017, **129**, 15264– 15268.
Wiley Online Library | Google Scholar | Get it at UC

31

31a T. Marcelli, H. Hiemstra, *Synthesis* 2010, **8**, 1229– 1279;
Crossref | CAS | Web of Science® | Google Scholar | Get it at UC

31b T. P. Yoon, E. N. Jacobsen, *Science* 2003, **299**, 1691– 1693;
Crossref | CAS | PubMed | Web of Science® | Google Scholar | Get it at UC

31c P. Melchiorre, *Angew. Chem. Int. Ed.* 2012, **51**, 9748– 9770;
Wiley Online Library | CAS | PubMed | Web of Science® | Google Scholar | Get it at UC
Angew. Chem. 2012, **124**, 9886– 9909;
Wiley Online Library | Google Scholar | Get it at UC

31d S.-K. Tian, Y. Chen, J. Hang, L. Tang, P. McDaid, L. Deng, *Acc. Chem. Res.* 2004, **37**, 621– 631;
Crossref | CAS | PubMed | Web of Science® | Google Scholar | Get it at UC

31e S.-S. Jew, H.-G. Park, *Chem. Commun.* 2009, 46, 7090– 7103;
Web of Science® | Google Scholar | Get it at UC

31f G. Bergonzini, S. Vera, P. Melchiorre, *Angew. Chem. Int. Ed.* 2010, **49**, 9685– 9688;
Wiley Online Library | CAS | PubMed | Web of Science® | Google Scholar | Get it at UC
Angew. Chem. 2010, **122**, 9879– 9882;
Wiley Online Library | Google Scholar | Get it at UC

31g C. G. Oliva, A. M. S. Silva, D. I. S. P. Resende, F. A. A. Paz, J. A. S. Cavaleiro, *Eur. J. Org. Chem.* 2010, 3449– 3458;
Wiley Online Library | CAS | Web of Science® | Google Scholar | Get it at UC

31h J. Duana, P. Li, *Catal. Sci. Technol.* 2014, **4**, 311– 320.
Crossref | Web of Science® | Google Scholar | Get it at UC

32

32a R. Mose, G. Preegel, J. Larsen, S. Jakobsen, E. H. Iversen, K. A. Jørgensen, *Nat. Chem.* 2017, **9**, 487–492;
Crossref | CAS | PubMed | Web of Science® | Google Scholar | Get it at UC

32b Z. Zhou, Z.-X. Wang, Y.-C Zhou, W. Xiao, Q. Ouyang, W. Du, Y.-C. Chen, *Nat. Chem.* 2017, **9**, 590–594;
Crossref | CAS | PubMed | Web of Science® | Google Scholar | Get it at UC

32c Y. Yang, Y. Jiang, W. Du, Y.-C. Chen, *Chem. Eur. J.* 2020, **26**, 1754– 1758.
Wiley Online Library | CAS | PubMed | Web of Science® | Google Scholar | Get it at UC

33 R. Mose, G. Preegel, J. Larsen, S. Jakobsen, E. H. Iversen, K. A. Jørgensen, *Nat. Chem.* 2017, **9**(5), 487– 492.

Crossref | CAS | PubMed | Web of Science® | Google Scholar | Get it at UC

34 P. Yu, C. Q. He, A. Simon, W. Li, R. Mose, M. K. Thøgersen, K. A. Jørgensen, K. N. Houk, *J. Am. Chem. Soc.* 2018, **140**, 13726– 13735.
Crossref | CAS | PubMed | Web of Science® | Google Scholar | Get it at UC

35 X. Chen, M. K. Thøgersen, K. Yang, R. F. Lauridsen, X.-S. Xue, K. A. Jørgensen, K. N. Houk, *J. Am. Chem. Soc.* 2021, 143, 934– 944.
Web of Science® | Google Scholar | Get it at UC

36

36a G. Bertuzzi, M. K. Thøgersen, M. Giardinetti, A. Vidal-Albalat, A. Simon, K. N. Houk, K. A. Jørgensen, *J. Am. Chem. Soc.* 2019, 141, 3288– 3297;
Web of Science® | Google Scholar | Get it at UC

36b D. V. Vidhani, J. R. Gillett, Y. Cusido, I. V. Alabugin *J. Phys. Chem. A* 2020, 124(9), 6016– 6028 and references therein.
Web of Science® | Google Scholar | Get it at UC

37 C. S. Jamieson, M. Ohashi, F. Liu, Y. Tang, K. N. Houk, *Nat. Prod. Rep.* 2019, **36**(5), 698– 713.
Crossref | CAS | PubMed | Web of Science® | Google Scholar | Get it at UC

38 S. Laschat, *Angew. Chem. Int. Ed. Engl.* 1996, **35**(3), 289– 291.
Wiley Online Library | CAS | Web of Science® | Google Scholar | Get it at UC

39 A. Ichihara, H. Oikawa, *Curr. Org. Chem.* 1998, **2**, 365– 394.
Crossref | CAS | Web of Science® | Google Scholar | Get it at UC

40 E. M. Stocking, R. M. Williams, *Angew. Chem. Int. Ed.* 2003, **42**(27), 3078– 3115.
Wiley Online Library | CAS | PubMed | Web of Science® | Google Scholar | Get it at UC

41 H. Oikawa, T. Tokiwano, *Nat. Prod. Rep.* 2004, **21**(3), 321– 352.
Crossref | CAS | PubMed | Web of Science® | Google Scholar | Get it at UC

42 P. R. Andrews, G. D. Smith, I. G. Young, *Biochemistry* 1973, **12**(18), 3492– 3498.
Crossref | CAS | PubMed | Web of Science® | Google Scholar | Get it at UC

43 H. Goerisch, *Biochemistry* 1978, **17**(18), 3700– 3705.
Crossref | CAS | PubMed | Web of Science® | Google Scholar | Get it at UC

44 Y. M. Chook, H. Ke, W. N. Lipscomb, *Proc. Nat. Acad. Sci.* 1993, **90**(18), 8600– 8603.
Crossref | CAS | PubMed | Web of Science® | Google Scholar | Get it at UC

45 J. V. Gray, J. R. Knowles, *Biochemistry* 1994, **33**(33), 9953– 9959.
Crossref | CAS | PubMed | Web of Science® | Google Scholar | Get it at UC

46 D. J. Gustin, P. Mattei, P. Kast, O. Wiest, L. Lee, W. W. Cleland, D. Hilvert, *J. Am. Chem. Soc.* 1999, **121**(8), 1756– 1757.
Crossref | CAS | Web of Science® | Google Scholar | Get it at UC

47 K. Katayama, T. Kobayashi, H. Oikawa, M. Honma, A. Ichihara, *Biochim. Biophys. Acta Protein Struct. Mol. Enzymol.* 1998, **1384**(2), 387– 395.
Crossref | CAS | PubMed | Web of Science® | Google Scholar | Get it at UC

48 H. Oikawa, T. Kobayashi, K. Katayama, Y. Suzuki, A. Ichihara, *J. Org. Chem.* 1998, **63**(24), 8748–8756.
Crossref | CAS | Web of Science® | Google Scholar | Get it at UC

49 D. J. Witter, J. C. Vederas, *J. Org. Chem.* 1996, **61**(8), 2613– 2623.
Crossref | CAS | PubMed | Web of Science® | Google Scholar | Get it at UC

50 K. Auclair, A. Sutherland, J. Kennedy, D. J. Witter, J. P. Van den Heever, C. R. Hutchinson, J. C. Vederas, *J. Am. Chem. Soc.* 2000, **122** (46), 11519– 11520.
Crossref | CAS | Web of Science® | Google Scholar | Get it at UC

51 S. M. Ma, J. W.-H. Li, J. W. Choi, H. Zhou, K. K. M. Lee, V. A. Moorthie, X. Xie, J. T. Kealey, N. A. Da Silva, J. C. Vederas, Y. Tang, *Science* 2009, **326**(5952), 589– 592.
Crossref | CAS | PubMed | Web of Science® | Google Scholar | Get it at UC

52 H. J. Kim, M. W. Ruszczycky, S. Choi, Y. Liu, H. Liu, *Nature* 2011, **473**, 109– 112.
Crossref | CAS | PubMed | Web of Science® | Google Scholar | Get it at UC

53 Z. Yang, S. Yang, P. Yu, Y. Li, C. Doubleday, J. Park, A. Patel, B. Jeon, W. K. Russell, H. Liu, D. H. Russell, K. N. Houk, *Proc. Nat. Acad. Sci.* 2018, **115**(5), E848- E855.
Crossref | CAS | PubMed | Web of Science® | Google Scholar | Get it at UC

54 M. G. Medvedev, A. A. Zeifman, F. N. Novikov, I. S. Bushmarinov, O. V. Stroganov, I. Y. Titov, G. G. Chilov, I. V. Svitanko, *J. Am. Chem. Soc.* 2017, **139**(11), 3942– 3945.
Crossref | CAS | PubMed | Web of Science® | Google Scholar | Get it at UC

55 C. D. Fage, E. A. Isiorho, Y. Liu, D. T. Wagner, H. Liu, A. T. Keatinge-Clay, *Nat. Chem. Biol.* 2015, **11**(4), 256– 258.
Crossref | CAS | PubMed | Web of Science® | Google Scholar | Get it at UC

56 A. Patel, Z. Chen, Z. Yang, O. Gutiérrez, H. Liu, K. N. Houk, D. A. Singleton, *J. Am. Chem. Soc.* 2016, **138**(11), 3631– 3634.
Crossref | CAS | PubMed | Web of Science® | Google Scholar | Get it at UC

57 B. A. Hess, L. Smentek, *Org. Biomol. Chem.* 2012, **10**(37), 7503– 7509.
Crossref | CAS | PubMed | Web of Science® | Google Scholar | Get it at UC

58 Z. Tian, P. Sun, Y. Yan, Z. Wu, Q. Zheng, S. Zhou, H. Zhang, F. Yu, X. Jia, D. Chen, A. Mándi, T. Kurtán, W. Liu, *Nat. Chem. Biol.* 2015, **11**(4), 259– 265.
Crossref | CAS | PubMed | Web of Science® | Google Scholar | Get it at UC

59 M. J. Byrne, N. R. Lees, L.-C. Han, M. W. van der Kamp, A. J. Mulholland, J. E. M. Stach, C. L. Willis, P. R. Race, *J. Am. Chem. Soc.* 2016, **138**(19), 6095– 6098.
Crossref | CAS | PubMed | Web of Science® | Google Scholar | Get it at UC

60 M. Sato, F. Yagishita, T. Mino, N. Uchiyama, A. Patel, Y.-H. Chooi, Y. Goda, W. Xu, N. Noguchi, T. Yamamoto, K. Hotta, K. N. Houk, Y. Tang, K. Watanabe, *ChemBioChem* 2015, **16**(16), 2294– 2298.
Wiley Online Library | CAS | PubMed | Web of Science® | Google Scholar | Get it at UC

61 M. Sato, S. Kishimoto, M. Yokoyama, C. S. Jamieson, K. Narita, N. Maeda, K. Hara, H. Hashimoto, Y. Tsunematsu, K. N. Houk, Y. Tang, K. Watanabe, *Nat. Catal.* 2021, **4**, 223– 232.
Crossref | CAS | Web of Science® | Google Scholar | Get it at UC

62 N. Kato, T. Nogawa, R. Takita, K. Kinugasa, M. Kanai, M. Uchiyama, H. Osada, S. Takahashi, *Angew. Chem. Int. Ed.* 2018, **57**(31), 9754– 9758.
Wiley Online Library | CAS | PubMed | Web of Science® | Google Scholar | Get it at UC

63 L. Li, P. Yu, M.-C. Tang, Y. Zou, S.-S. Gao, Y.-S. Hung, M. Zhao, K. Watanabe, K. N. Houk, Y. Tang, *J. Am. Chem. Soc.* 2016, **138**(49), 15837– 15840.
Crossref | CAS | PubMed | Web of Science® | Google Scholar | Get it at UC

64 D. Tan, C. S. Jamieson, M. Ohashi, M. C. Tang, K. N. Houk, Y. Tang, *J. Am. Chem. Soc.* 2019, **141**(2), 769– 773.
Crossref | CAS | PubMed | Web of Science® | Google Scholar | Get it at UC

65 M. Ohashi, F. Liu, Y. Hai, M. Chen, M. Tang, Z. Yang, M. Sato, K. Watanabe, K. N. Houk, Y. Tang, *Nature* 2017, **549**, 502– 506.
Crossref | PubMed | Web of Science® | Google Scholar | Get it at UC

66 Y. Cai, Y. Hai, M. Ohashi, C. S. Jamieson, M. Garcia-Borras, K. N. Houk, J. Zhou, Y. Tang, *Nat. Chem.* 2019, **11**(9), 812– 820.
Crossref | CAS | PubMed | Web of Science® | Google Scholar | Get it at UC

67 Z. Zhang, C. S. Jamieson, Y.-L. Zhao, D. Li, M. Ohashi, K. N. Houk, Y. Tang, *J. Am. Chem. Soc.* 2019, **141**(14), 5659– 5663.
Crossref | CAS | PubMed | Web of Science® | Google Scholar | Get it at UC

68 B. Zhang, K. B. Wang, W. Wang, X. Wang, F. Liu, J. Zhu, J. Shi, L. Y. Li, H. Han, K. Xu, H. Y. Qiao, X. Zhang, R. H. Jiao, K. N. Houk, Y. Liang, R. S. Tan, H. M. Ge, *Nature* 2019, **568**(7750), 122– 126.
Crossref | CAS | PubMed | Web of Science® | Google Scholar | Get it at UC

69 R. Schor, C. Schotte, D. Wibberg, J. Kalinowski, R. J. Cox, *Nat. Commun.* 2018, **9**(1), 69 Article *Number* 1963.
Crossref | PubMed | Web of Science® | Google Scholar | Get it at UC

70 Q. Chen, J. Gao, C. Jamieson, J. Liu, M. Ohashi, J. Bai, D. Yan, B. Liu, Y. Che, Y. Wang, K. N. Houk, Y. Hu, *J. Am. Chem. Soc.* 2019, **141**(36), 14052– 14056.
Crossref | CAS | PubMed | Web of Science® | Google Scholar | Get it at UC

71 L. Gao, C. Su, X. Du, R. Wang, S. Chen, Y. Zhou, C. Liu, X. Liu, R. Tian, L. Zhang, K. Xie, S. Chen, Q. Guo, L Guo, Y. Hano, M. Shimazaki, A. Minami, H. Oikawa, N. Huang, K. N. Houk, L. Huang, J. Dai, X. Lei, *Nat. Chem.* 2020, **12**(7), 620– 628.
Crossref | CAS | PubMed | Web of Science® | Google Scholar | Get it at UC

72 M. Ohashi, C. S. Jamieson, Y. Cai, D. Tan, D. Kanayama, M.-C. Tang, S. M. Anthony, J. V. Chari, J. S. Barber, E. Picazo, T. B. Kakule, S. Cao, N. K. Garg, J. Zhou, K. N. Houk, Y. Tang, *Nature* 2020, **586**(7827), 64– 69.
Crossref | CAS | PubMed | Web of Science® | Google Scholar | Get it at UC

73 M. S. DeClue, K. K. Baldridge, D. E. Künzler, P. Kast, D. Hilvert, *J. Am. Chem. Soc.* 2005, **127**(43),

15002– 15003.
Crossref | CAS | PubMed | Web of Science® | Google Scholar | Get it at UC

74 Y. Katsuyama, X.-W. Li, R. Müller, B. Nay, *ChemBioChem* 2014, **15**(16), 2349– 2352.
Wiley Online Library | CAS | PubMed | Web of Science® | Google Scholar | Get it at UC

75 L. W. Shipman, D. Li, C. A. Roessner, A. I. Scott, J. C. Sacchettini, *Structure* 2001, **9**(7), 587– 596.
Crossref | CAS | PubMed | Web of Science® | Google Scholar | Get it at UC

76 S. A. Newmister, S. Li, M. Garcia-Borràs, J. N. Sanders, S. Yang, A. N. Lowell, F. Yu, J. L. Smith, R. M. Williams, K. N. Houk, D. H. Sherman, *Nat. Chem. Biol.* 2018, **14**(4), 345– 351.
Crossref | CAS | PubMed | Web of Science® | Google Scholar | Get it at UC

77 Q. Zhu, X. Liu, *Angew. Chem. Int. Ed.* 2017, **56**(31), 9062– 9066.
Wiley Online Library | CAS | PubMed | Web of Science® | Google Scholar | Get it at UC

Biographical Information

K. N. Houk is Distinguished Research Professor at UCLA. He received his Ph.D. in 1968 with R. B. Woodward. Houk is an authority on computational organic chemistry and collaborates with experimental research groups all over the world. He is is a member of the US National Academy of Sciences and recently was awarded the Roger Adams Award by the Organic Division of the American Chemical Society.

Biographical Information

Xiao-Song Xue received his Ph.D. at Nankai University (NKU) in 2013 with Jin-Pei Cheng. He joined the College of Chemistry at NKU as an assistant professor and was promoted to associate professor in 2016. He was a visiting scholar at the Department of Chemistry and Biochemistry at UCLA with K. N. Houk from 2017 to 2020. His research interests including chemical bonding, reaction mechanisms, and physical organofluorine chemistry.

Biographical Information

Cooper S. Jamieson received a BA in Chemistry and a BA in Art from Lewis & Clark College in Portland, OR in 2016. Upon graduation, he moved to far-West Marfa, Texas and worked in art conservation at the Chinati Foundation. Currently, he is finishing his Ph.D. under the direction of Prof. K. N. Houk and Prof. Yi Tang at the University of California, Los Angeles. Cooper's research is at the interface of computational chemistry and biochemistry, where he has discovered a new family of enzymes, the pericyclases, that catalyze classic organic reactions in nature.

Biographical Information

Fang Liu received her B.S. in chemistry from Nankai University, China, in 2009. She received her Ph.D. with K. N. Houk at UCLA in 2014, studying gating in container molecules and the factors controlling reactivity in bioorthogonal cycloadditions. She continued at UCLA as a postdoctoral fellow in the Houk group and a postdoctoral fellow in the Liang group at Nanjing University. She is now a professor at Nanjing Agricultural University, China, and chief designer/artist of DesignOne, a scientific design studio.

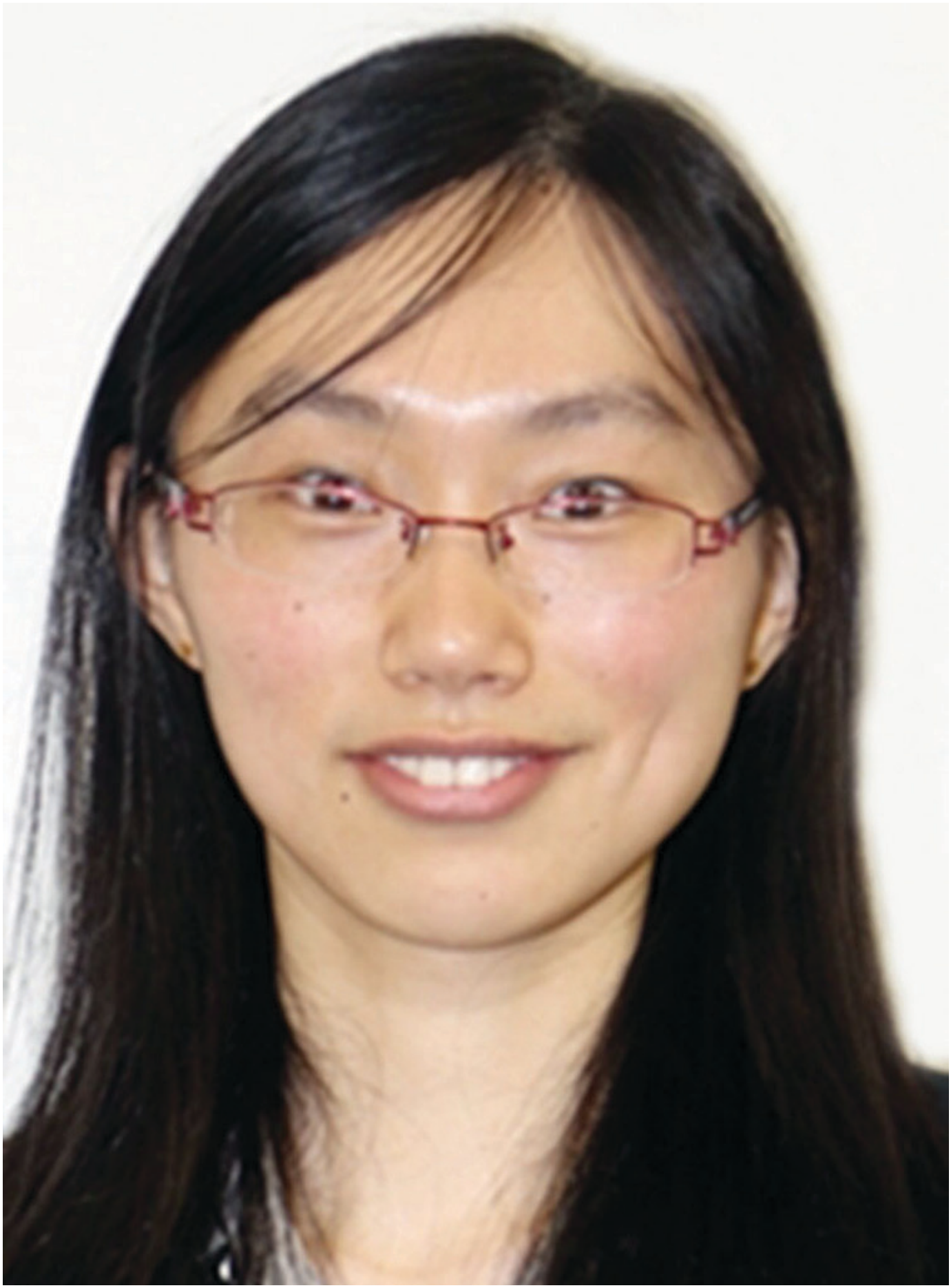

Biographical Information

Yu Chen received his bachelor's and Master's degrees from Jilin University (China) in 2011 and 2015. He has been a research assistant at Nanjing University since 2016, working with Prof. Yong Liang. Yu Chen's research focuses on the mechanism of catalytic processes promoted by organic molecules, metal complexes, enzymes, and design of highly efficient catalysts using calculational chemistry.

Biographical Information

Xiangyang Chen (1988) received her B.S. degree in Applied Chemistry from Shandong Normal University in 2011, her M.S. degree in Physical Chemistry from Capital Normal University in 2014, and her Ph.D. degree from the Institute of Chemistry, Chinese Academy of Sciences in 2017. She then joined the group led by Professor K. N. Houk in 2017 at University of California, Los Angeles to be a postdoc. Her research focuses on computational studies of organometallic reactions with an emphasis on elucidating reaction mechanisms and the role of ligand and the nature of the selectivity.

Citing Literature

Download PDF